

Disentangling the impact of catchment heterogeneity on nitrate export dynamics from event to long-term time scales

Carolin Winter¹, Stefanie Lutz², Andreas Musolff³, Rohini Kumar⁴, Michael Weber⁵, and Jan Fleckenstein⁶

¹UFZ - Helmholtz Centre for Environmental Research

²UFZ Helmholtz Centre for Environmental Research

³UFZ - Helmholtz-Centre for Environmental Research

⁴UFZ-Helmholtz Centre for Environmental Research

⁵UFZ-Helmholtz Center for Environmental Research

⁶Helmholtz Center for Environmental Research - UFZ

November 22, 2022

Abstract

Defining effective measures to reduce nitrate pollution in heterogeneous mesoscale catchments remains challenging if based on concentration measurements at the outlet only. One reason is our limited understanding of the sub-catchment contributions to nitrate export and their importance at different time scales. While upstream sub-catchments often disproportionately contribute to runoff generation and in turn to nutrient export, agricultural areas, which are typically found in downstream lowlands, are known to be a major source for nitrate pollution. To disentangle the interplay of these contrasting drivers of nitrate export, we analyzed seasonal long-term trends and event dynamics of nitrate concentrations, loads and the concentration-discharge relationship in three nested catchments within the Selke catchment (456 km²), Germany. The upstream sub-catchments (40.4 % of total catchment area, 34.5 % of N input) had short transit times and dynamic concentration-discharge relationships with elevated nitrate concentrations during wet seasons and events. Consequently, the upstream sub-catchments dominated nitrate export during high flow and disproportionately contributed to overall annual nitrate loads at the outlet (64 %). The downstream sub-catchment was characterized by higher N input, longer transit times and relatively constant nitrate concentrations between seasons, dominating nitrate export during low flow periods. Neglecting the disproportional role of upstream sub-catchments for temporally elevated nitrate concentrations and net annual loads can lead to an overestimation of the role of agricultural lowlands. Nonetheless, in agricultural lowlands, constantly high concentrations from nitrate legacies pose a long-term threat to water quality. This knowledge is crucial for an effective and site-specific water quality management.

1
2 **Disentangling the impact of catchment heterogeneity on nitrate export dynamics**
3 **from event to long-term time scales**
4

5 **Carolin Winter^{1*}, Stefanie R. Lutz¹, Andreas Musolff¹, Rohini Kumar², Michael Weber²,**
6 **and Jan H. Fleckenstein^{1,3}**

7 ¹Department for Hydrogeology, Helmholtz Centre for Environmental Research - UFZ, 04318
8 Leipzig, Germany

9 ²Department for Computational Hydrosystems, Helmholtz Centre for Environmental Research -
10 UFZ, 04318 Leipzig, Germany

11 ³Bayreuth Center of Ecology and Environmental Research, University of Bayreuth, 95440
12 Bayreuth, Germany

13 Corresponding author: Carolin Winter (carolin.winter@ufz.de)
14

15 **Key Points:**

- 16
- 17 • Analyzing the CQ-relationship across time scales allows to disentangle the impact of
catchment heterogeneity on nitrate export.
 - 18 • Mountainous upstream sub-catchments can dominate nitrate export during high flows and
19 disproportionally contribute to nitrate loads.
 - 20 • Agricultural downstream sub- catchments can dominate nitrate export during low flow
21 and pose a long-term threat to water quality.

Abstract

Defining effective measures to reduce nitrate pollution in heterogeneous mesoscale catchments remains challenging if based on concentration measurements at the outlet only. One reason is our limited understanding of the sub-catchment contributions to nitrate export and their importance at different time scales. While upstream sub-catchments often disproportionately contribute to runoff generation and in turn to nutrient export, agricultural areas, which are typically found in downstream lowlands, are known to be a major source for nitrate pollution. To disentangle the interplay of these contrasting drivers of nitrate export, we analyzed seasonal long-term trends and event dynamics of nitrate concentrations, loads and the concentration-discharge relationship in three nested catchments within the Selke catchment (456 km²), Germany. The upstream sub-catchments (40.4 % of total catchment area, 34.5 % of N input) had short transit times and dynamic concentration-discharge relationships with elevated nitrate concentrations during wet seasons and events. Consequently, the upstream sub-catchments dominated nitrate export during high flow and disproportionately contributed to overall annual nitrate loads at the outlet (64.2 %). The downstream sub-catchment was characterized by higher N input, longer transit times and relatively constant nitrate concentrations between seasons, dominating nitrate export during low flow periods. Neglecting the disproportional role of upstream sub-catchments for temporally elevated nitrate concentrations and net annual loads can lead to an overestimation of the role of agricultural lowlands. Nonetheless, in agricultural lowlands, constantly high concentrations from nitrate legacies pose a long-term threat to water quality. This knowledge is crucial for an effective and site-specific water quality management.

Plain Language Summary

To efficiently remove nitrate pollution we need to understand how it is transported, mobilized and stored within large and heterogeneous catchments. Former studies show that upstream catchments often have a disproportional impact on nutrient export, while agriculture, a major nitrate source, is often located at downstream lowlands. To understand which parts of a catchment contribute most to nitrate export and when, we analyzed long-term (1983-2016) and high-frequency (2010-2016) data in the Selke catchment (Germany) at three locations. The mountainous upstream part dominated nitrate transport during winter, spring and rain events. It had a surprisingly high contribution to annual nitrate loads. The agricultural downstream part of the catchment dominated nitrate export during summer and autumn with relatively constant concentrations between seasons. Here, nitrogen inputs need more than a decade to travel through the subsurface of the catchment, which causes a time lag between measures to reduce nitrate pollution and their measurable effect. The resulting storage of nitrate in the groundwater threatens drinking water quality for decades to come. While the role of agricultural lowlands for nitrate export can be overestimated if neglecting the disproportional role of upstream sub-catchments, their impact poses a long-term threat to water quality.

59

60

61

62

63 1 Introduction

64 High nitrate concentrations in ground- and surface water are a long-known but still
65 widespread problem in most developed countries (Bouraoui & Grizzetti, 2011; Kohl et al., 1971;
66 Rockström et al., 2009). These high concentrations pose a threat to our drinking water quality
67 and the integrity of aquatic ecosystems (Camargo & Alonso, 2006; Majumdar & Gupta, 2000).
68 To most efficiently reduce nitrate pollution, a detailed understanding of the catchment-internal
69 processes that drive nitrate mobilization, transport, storage and decay is needed. While good
70 knowledge about these processes exists for rather uniform headwater catchments, understanding
71 those in spatially more heterogeneous and complex mesoscale catchments ($10^1 - 10^4$ km², Breuer
72 et al., 2008) is yet an open challenge, but vital for identifying management options. Upstream
73 sub-catchments, on the one hand, often have a disproportional contribution to runoff generation
74 due to their higher drainage density and in turn they often disproportionately contribute to nutrient
75 mobilization and transport (e.g. Alexander et al., 2007; Dodds & Oakes, 2008; Goodridge &
76 Melack, 2012). Agricultural areas, on the other hand, are known to be a major source area for
77 nitrate pollution (e.g. Padilla et al., 2018; Strebel et al., 1989). A typical setting for many
78 mesoscale catchments in European uplands is, however, an elevated upstream area with no or a
79 small percentage of agricultural land use and a downstream lowland area where agricultural land
80 use dominates (e.g. Krause et al., 2006; Montzka et al., 2008). Hence, the different upstream and
81 downstream sub-catchments can have quite different nitrate export dynamics, which are both
82 relevant for nitrate export from the entire catchment and which may operate at very different
83 times and time-scales. Their specific contribution, however, remains widely unknown if
84 measuring only the integrated signal of nitrate export at the catchment's outlet, which makes it
85 difficult to localize important source zones of nitrate and to identify important driving forces for
86 their mobilization. To solve this issue, nested catchment studies are a promising approach to shed
87 light on the contribution from sub-catchments to nitrate export (e.g. Dupas et al., 2017; Ehrhardt
88 et al., 2019). They enable to analyze changes in nitrate transport along the river and to connect
89 these changes to the specific characteristics of upstream and downstream sub-catchments and to
90 interpret the integrated observations of concentration, Q and loads at the catchment outlet.

91 1.1 Time scales of nitrate export

92 The dynamics of water quality can be assessed on various time scales, which all have
93 their specific relevance for understanding nitrate export dynamics at catchment scale. Long-term
94 data are indispensable to assess trends in water quality over time and to assess transit times
95 (TTs) and legacy stores, which can delay or buffer the catchment response to solute input at the
96 catchment outlet (Dupas et al., 2016; Hirsch et al., 2010; Van Meter et al., 2017). Here, we refer
97 to TTs as the time lag between a solute being introduced into the catchment and its riverine
98 export. TTs of nitrate can vary between <1 year and up to >50 years, strongly dependent on the
99 catchment characteristics and dominant flow paths (Ehrhardt et al., 2019; Van Meter et al.,
100 2017). Legacy stores refer to the mass of solute – in our case nitrate – that has been retained and
101 accumulated in the catchment. In the case of nitrate they are separated in organic N retained in
102 the soil (biogeochemical legacy) and in inorganic N that is moving in the groundwater with long
103 TTs (hydrological legacy). A precise understanding of these processes – TTs and legacy stores –
104 is still missing. However, this knowledge is crucial to understand the response of riverine nitrate
105 concentrations to land use changes and the time scale between measures to reduce nitrate
106 reduction and their measurable success. Moreover, understanding the controls on the long-term

107 persistence of pollutants - such as nitrate - within catchments was just recently framed to be one
108 of the major unsolved problems in hydrology (Blöschl et al., 2019).

109 Long-term data are most often available at a low frequency (weekly to monthly), because
110 methods to continuously measure high-frequency nitrate concentrations have been developed
111 only recently (Burns et al., 2019). While these long-term low-frequency data are appropriate for
112 the identification of long-term trends, TTs and legacy stores (e.g. Ehrhardt et al., 2019; Hirsch et
113 al., 2010), the analysis of event dynamics can only be conducted with high-frequency data
114 (Burns et al., 2019). The time scale of single events, however, is especially important for the
115 analysis of nitrate dynamics, because most of the annual nitrate load to the stream is transported
116 during events (Bernal et al., 2002; Inamdar et al., 2006). Event dynamics of nitrate
117 concentrations (C) and Q can shed light on mobilization and transport processes that are masked
118 if looking at long-term trends only (Duncan et al., 2017; Rose et al., 2018). For example, Dupas
119 et al. (2016) found chemostasis (variability of nitrate concentrations is low compared to that of Q
120 and there is no significant directional relationship between C and Q) in long-term trends in a
121 mesoscale catchment, while dynamics at the scale of single discharge events conversely showed
122 a decrease of nitrate concentrations with increasing Q. They argued that these event-scale
123 patterns are one of the main drivers for the uncertainty in annual load estimations. Moreover,
124 both long-term trends and event dynamics often show a strong seasonality (e.g. Dupas et al.,
125 2017), which should be analyzed in parallel to accurately assess nitrate export patterns across
126 time scales. Consequently, a combination of analyses of all - long-term trends, event dynamics
127 and their seasonality - is needed to address the knowledge gap in driving forces of nitrate export
128 dynamics.

129 1.2 Concentration-discharge relationship

130 The concentration-discharge relationship (CQ-relationship) is a simple data-driven
131 concept that is commonly used to investigate export dynamics of nitrate or other solutes at
132 various spatial and temporal scales (e.g. Godsey et al., 2009; Musolff et al., 2015; Rose et al.,
133 2018). In general, the CQ-relationship allows to differentiate between three different export
134 regimes: i) chemodynamic with accretion pattern, ii) chemodynamic with dilution pattern and iii)
135 chemostasis (Godsey et al., 2009; Musolff et al., 2017). Export regimes i) and ii) are both
136 summarized under the term “chemodynamic”, which means that a solute’s concentration
137 variability is comparable or higher than the variability of Q, with concentrations either increasing
138 (accretion) or decreasing (dilution) with increasing Q. Accretion patterns are generally explained
139 by additional source zones getting connected during higher flow conditions, while dilution
140 patterns are observed when higher Q causes a dilution of instream solute concentrations without
141 further source zone activation (Basu et al., 2010). Chemodynamic nitrate export has often been
142 found in relatively natural systems with no or only a small percentage of agricultural land use or
143 urban areas, where nitrate sources are not ubiquitously available (Basu et al., 2010; Goodridge &
144 Melack, 2012). On the contrary, chemostasis indicates constant nutrient concentrations in-stream
145 that are not significantly correlated to Q and have a considerably lower variability (Basu et al.,
146 2010; Bieroza et al., 2018). This pattern often emerges in catchments with a spatially uniform
147 distribution of abundant solute sources, such as nitrate in agricultural areas, leading to a
148 relatively constant release of solutes to the stream network (Basu et al., 2010; Bieroza et al.,
149 2018). To assess the directional relationship between C and Q, Godsey et al. (2009) proposed a
150 power law relationship between C and Q with the corresponding slope between $\ln(C)$ and $\ln(Q)$ –
151 termed the CQ-slope. Subsequently, Thompson et al. (2011) established the CV_C/CV_Q metric to

152 express the variability in C relative to the variability in Q (with CV being the coefficient of
153 variation). Jawitz & Mitchell (2011) and Musolff et al. (2015) combined both approaches to a
154 single conceptual framework as CQ-slope and CV_C/CV_Q are mathematically linked.

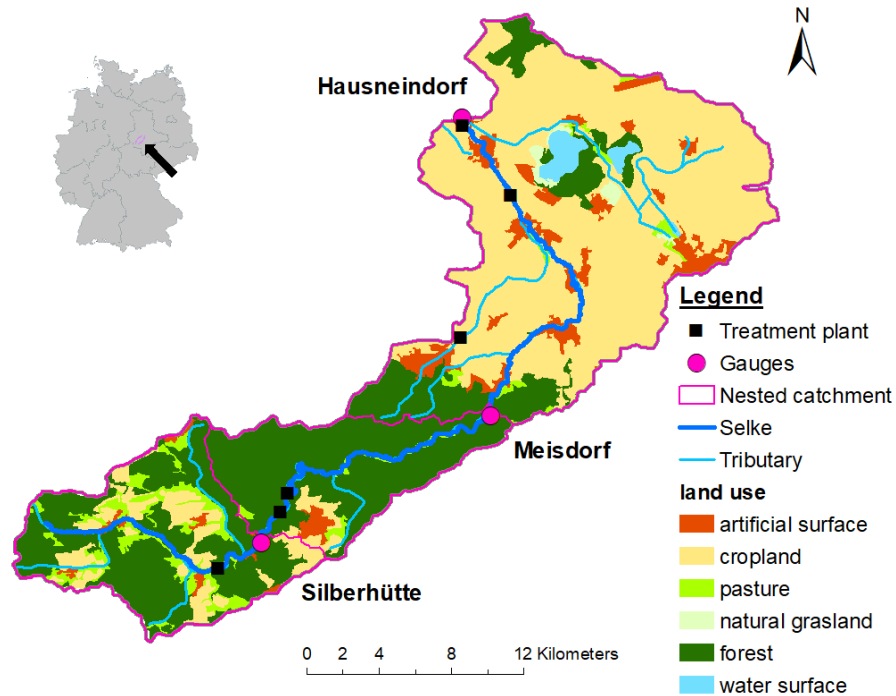
155 So far, top down assessments of catchment export dynamics have mainly been focused on
156 observations at the catchment outlet, largely neglecting catchment internal variabilities. Here we
157 see a need for research on how the role of internal organization of catchments (i.e., nested sub-
158 catchments) in term of nitrate inputs, reactive transport in the subsurface and the stream network,
159 shapes the outlet observation seasonally and under varying flow conditions. To address this
160 research gap, we conduct a nested catchment study in the mesoscale Selke catchment, which is
161 an intensively monitored research site (Jiang et al., 2014; Wollschläger et al., 2017) and provides
162 the unique opportunity to study long-term trends as well as event-scale nitrate concentrations and
163 loads. We analyzed i) seasonal long-term trends and ii) event dynamics of nitrate concentrations,
164 loads and the CQ-relationship for each nested sub-catchment. Furthermore, we iii) calculated
165 sub-catchment specific transit time distributions (TTDs) from N inputs and riverine nitrate
166 outputs to discuss the potential extent and effect of legacy stores and their impact on nitrate
167 export dynamics and long-term trends. With this comprehensive approach, we aim at a better
168 understanding of how nested sub-catchments i) compose the integrated response of nitrate
169 concentrations, loads and CQ-relationships observed at the catchment outlet at different times
170 scales (long-term, seasonal and event scale); and ii) affect the response of nitrate concentrations,
171 loads and CQ-relationships to changes in N input.

172 **2 Materials and Methods**

173 **2.1 Catchment description**

174 The Selke catchment is located in the Harz Mountains and the Harz foreland of Saxony-
175 Anhalt, Germany (Fig.1). It is a sub-catchment of the Bode catchment, which is an intensively
176 monitored catchment within the network of TERrestrial ENVironmental Observatories
177 (TERENO, Wollschläger et al., 2017). Within the Selke catchment, we consider three nested
178 sub-catchments (Fig. 1), delineated by the following gauging stations: i) Silberhütte, with a
179 drainage area of 105 km², ii) Meisdorf (184 km²) and iii) Hausneindorf (456 km²). Daily average
180 specific Q is 0.90 mm d⁻¹, 0.65 mm d⁻¹ and 0.32 mm d⁻¹ for Silberhütte, Meisdorf and
181 Hausneindorf, respectively.

182 Silberhütte and Meisdorf are located in the Harz Mountains and drain the upper part of
183 the catchment. In the following, these two nested sub-catchments are summarized as the *upper*
184 *Selke*. In the upper Selke, forests are the dominant land use (73 %), followed by agriculture
185 (21 %), which is mainly located upstream of Silberhütte. Soils are dominated by Cambisols
186 overlaying low permeable schist and claystone, resulting in relatively shallow groundwater
187 systems (Jiang et al., 2014). Long-term mean precipitation is 694 mm a⁻¹ (based on the gridded
188 German Weather Service (DWD) datasets from Zink et al., 2017). There are three wastewater
189 treatment plants (WWTPs) located in the upper Selke, of which one is located at the upper part
190 draining to the gauge in Silberhütte.



191
 192 **Figure 1.** Land use map of the Selke catchment with gauging stations (pink dots) and wastewater
 193 treatment plants (black squares).
 194

195 The transition from the upper to the lower part of the catchment marks a distinct change
 196 in landscape characteristics. The downstream part of the catchment is termed *lower Selke* from
 197 here on. It is a fertile plain with productive soils in the foreland of the Harz Mountains
 198 dominated by agriculture (65 %) mainly in the form of arable crops. The long-term average
 199 precipitation is 519 mm. Soils are dominated by Chernozems above quaternary sediments and
 200 mesozoic sedimentary rocks (sandstone and limestone) that allow for considerably deeper
 201 groundwater systems, compared to the upper Selke (Jiang et al. 2014).

202 Another three WWTPs are located in the lower Selke, of which one is at a tributary to the
 203 Selke (Fig. 1). Furthermore, an opencast mine is located in the northeastern part of the lower
 204 Selke. After closing down the mine in 1991, Selke water was abstracted from 1998 on to fill the
 205 open pit with an average annual abstraction rate of 3.1 million m³. In 2009 a landslide occurred
 206 from the banks of the pit-lake so that since 2010 water from the filling pit has been pumped into
 207 the Selke in order to stabilize the banks (annual rate of 10.4 million m³).

208 Note that due to the nested catchment structure, all measurements from the lower Selke
 209 are an integrated signal from the upper and the lower Selke.

210 2.2 Data basis

211 Daily Q data are publicly available for all gauges from 1983 to 2016 on a daily basis and
 212 on a 15 min basis since 2010, provided by the State Office of Flood Protection and Water
 213 Management of Saxony-Anhalt (LHW; Fig. S1). Long-term data of nitrate concentrations for all
 214 three gauges were provided by the LHW from 1983 to 2009 and by the Helmholtz Centre for
 215 Environmental Research (UFZ) from 2010 to 2016, collected as grab samples at a biweekly to

216 bimonthly basis and published previously by Yang et al. (2018). Continuous high-frequency data
 217 of nitrate were measured in more recent years at 15 min intervals, using TriOS ProPS-UV
 218 sensors, described in more detail by Rode et al. (2016). The data were collected by the UFZ as
 219 part of the TERENO monitoring program from 2013 to 2016 for Silberhütte, October 2010 to
 220 2016 for Meisdorf and July 2010 to 2016 for Hausneindorf. Slight variations in the timing of
 221 measurements between Q and nitrate concentrations were corrected by aggregation to equal 15
 222 min intervals.

223 2.3 Long-term trends of concentrations and concentration-discharge relationships

224 All analyses were carried out within the R software environment (R Core Team, 2019).
 225 Long-term trends in nitrate concentrations and loads were calculated using ‘*Weighted Regression*
 226 *on Time, Discharge and Season*’ (WRTDS, Hirsch et al., 2010), implemented in the R-package
 227 ‘*Exploration and Graphics for RivEr Trends*’ (EGRET). WRTDS requires time, Q and season as
 228 explanatory variables to simulate daily concentrations from sporadic measurements over long
 229 time series (Hirsch et al., 2010):

$$230 \quad \ln(C_i) = \beta_{0,i} + \beta_{1,i}t_i + \beta_{2,i}\ln(Q_i) + \beta_{3,i}\sin(2\pi t_i) + \beta_{4,i}\cos(2\pi t_i) + \varepsilon_i \quad (1)$$

231 where subscript i indicates the specific day, C is the concentration in mg L^{-1} , t is the time
 232 in decimal years, Q is the discharge in $\text{m}^3 \text{s}^{-1}$, $\beta_1 - \beta_4$ are fitted coefficients with β_2 representing
 233 the CQ-slope and ε is an error term.

234 The regression in WRTDS is weighted via the tricube weight function (Tuckey, 1977),
 235 which gives an increasing relevance to observations close to the estimation point in terms of
 236 time, Q and season (Hirsch et al., 2010). Flow normalization is applied for an estimation of
 237 concentration that is unbiased by daily Q variation. Here, concentrations are flow-normalized
 238 (FN) in such a way that measured Q on a given date is assumed to have the same probability as
 239 all observed Q values of that date in all other years in the record. Thus, for every single date in
 240 the time series, eq. 1 is applied once with every Q record that was measured on the same date in
 241 all years and these values are finally averaged to one single FN concentration estimate for the
 242 specific day.

243 In order to analyze long-term trends of the CQ-relationship, we used a modification of
 244 the original EGRET codes to extract the daily parameter β_2 from eq. 1, which was developed by
 245 Zhang et al. (2016). The parameter β_2 represents the relationship between $\ln(C)$ and $\ln(Q)$ (CQ-
 246 slope), which enables a differentiation between export regimes: i) chemodynamic with an
 247 accretion pattern ($\beta_2 > 0.1$); ii) chemodynamic with a dilution pattern ($\beta_2 < -0.1$); and iii)
 248 chemostatic ($-0.1 < \beta_2 < 0.1$). We chose the threshold for chemostatic at -0.1 and 0.1 according
 249 to Zhang et al. (2016) and Bieroza et al. (2018) being aware that this somewhat arbitrary
 250 threshold only indicates chemostatic patterns if $CV_C/CV_Q \ll 1$ (Musolff et al., 2015). For nitrate,
 251 the CQ-slope and the CV_C/CV_Q were found to be positively correlated (Musolff et al., 2015) as
 252 most of the variability in C is explained by variability in Q . In this case, the additional
 253 information gained by the CV_C/CV_Q metric is small. Methods and results of this study are
 254 therefore restricted the CQ-slope only.

255 Using daily streamflow data and low-frequency nitrate concentrations, we calculated
 256 seasonally averaged and FN nitrate concentrations, loads and FN CQ-slopes for all gauges from
 257 1983 to 2016 in order to detect long-term trends and seasonal differences. Seasons were defined

258 as spring lasting from March to May, summer from June to August, autumn from September to
259 November and winter lasting from December to February. To quantify the uncertainty, all results
260 were bootstrapped 200 times using the R package EGRETci (Hirsch et al., 2015) for FN nitrate
261 concentrations and loads and a modification of the code from Zhang et al. (2016) for
262 bootstrapping β_2 . As recommended by Hirsch et al. (2015), we used a block length of 200
263 (randomly selected with replacement) and show the 90 % confidence interval in all consequent
264 figures (5 % - 95 % quantiles).

265 2.4 Nitrogen input

266 Nitrogen (N) input into the Selke catchment was calculated following the procedure
267 described by Ehrhardt et al. (2019). Here, N input refers to N surplus as the sum of three
268 different input classes: i) agricultural N surplus, ii) atmospheric N deposition, and iii) N input
269 from WWTPs, where i) and ii) are diffuse sources and iii) is a point source. To stay consistent
270 with the nested catchment structure, N input data of Meisdorf represents N input for the entire
271 upper Selke and N input from the lower Selke represents the entire Selke catchment, including
272 the upper part.

273 We used agricultural N surplus data derived for the 403 counties in Germany,
274 representing the annual surplus of N on agricultural areas that results from the difference
275 between N sources (i.e., fertilizer and manure application, atmospheric deposition and biological
276 N fixation by legumes) and N sinks in the form of N in harvested crops (Bach & Frede, 1998;
277 Häußermann et al., 2019). Our study area is covered by two counties. The share of agricultural
278 area for each county was taken from the CORINE Land Cover (CLC, EEA, 2012) for the years
279 1990, 2000, 2006 and 2012 and further corrected according to Bach et al. (2006 and pers. com),
280 introducing a scaling factor for each county to adjust for the mismatch between the CLC derived
281 agricultural share and that from statistical data sources (Bach et al., 2006).

282 Atmospheric N deposition represents the annual input from N emissions due to burning
283 in private households, industry and traffic between 1980 and 2015, provided by the
284 Meteorological Synthesizing Centre – West (MSC-W) of the European Monitoring and
285 Evaluation Programme EMEP (e.g. Bartnicky & Benedictow, 2017; Bartnicky & Fagerli, 2004).
286 From 1950 to 1980, a constant input is assumed, due to a lack of further data for that time. We
287 considered N deposition for the non-agricultural land cover classes (e.g. forest, water bodies,
288 wetlands, grassland) as the agricultural N surplus data already account for atmospheric
289 deposition (see above) and added the biological N fixation according to Cleveland et al. (1999)
290 and van Meter et al. (2017). Cities were neglected (except urban grassland like parks) under the
291 assumption that nitrogen from sealed surfaces is directly discharged into the WWTPs.

292 Annual mean nitrate and ammonium concentrations from WWTP outflow between 2010
293 and 2015 were provided by the Ministry of Environment, Agriculture and Energy Saxony-Anhalt
294 (MULE). We calculated nitrate input from WWTPs with the provided nitrate concentrations and
295 an additional maximum estimate for the contribution of WWTPs to nitrate export under the
296 assumption of a complete nitrification of wastewater-borne ammonium. For all years previous to
297 2010, nitrate concentrations from 2010 were assigned. We consider that these data and their
298 extrapolation robustly represent the recent state of point source N loads but do not allow for
299 describing the long-term evolution of N loads due to improvements in wastewater treatment and
300 newly constructed WWTPs.

301 Finally, a harmonized and consistent dataset for each of the three different input types
302 was created on county level (average area of 887 km²) for the period of 1950-2015 and combined
303 to one single N input dataset that was clipped for all three nested sub-catchments. To this end,
304 we used the weighted average, taking into account the areal fractions of involved counties and
305 the respective (sub-)catchment boundaries.

306 2.5 Transit time distributions

307 Apparent transit time distributions (TTDs) for nitrate were calculated applying a
308 methodology described by Musolff et al. (2017) and Ehrhardt et al. (2019). We assumed a log-
309 normal form for the TTDs because this allows to account for the long tails in the TTD needed to
310 adequately reflect legacy effects. First, we scaled N input and mean annual FN nitrate
311 concentrations from the long-term low-frequency data in order to compare the temporal
312 dynamics of input and output independently from their absolute value. Then, we calibrated the
313 parameters μ and σ of the log-normal distribution by minimizing the sum of squared errors
314 between simulated and measured scaled FN nitrate concentrations. We used these TTDs to
315 compare the response of the nested catchments to changes in N input and to improve our
316 estimate of N legacies in the period from 1983 to 2015. More specifically, we calculated the
317 total conservative N export for each sub-catchment by convolving the annual N input for each
318 year with the calibrated TTDs, extracting the fractions that would be exported by 2015, and
319 summing up these annual estimates to derive the cumulative N export until 2015. We then
320 compared this estimate of conservative N export to the measured nitrate export over the same
321 period to get an estimate of the *missing N*. We assume that missing N was either removed via
322 denitrification or it is still in the catchment as hydrological or biogeochemical legacy. A clear
323 separation of these two forms of legacies is challenging (Ehrhardt et al., 2019) and beyond the
324 scope of this study. Nevertheless, we used the long-term trends in the CQ-slope to discuss the
325 likely domination of either hydrological or biogeochemical legacies and compared the difference
326 between TTD-derived and measured N export to literature data on potential denitrification.

327 2.6 Event dynamics

328 We used the high-frequency data from 2010 to 2016 to analyze storm events at all three
329 gauges. To identify events, we converted Q from m³ s⁻¹ to mm, smoothed it with a running
330 average and separated it into a base flow and fast flow component following the methodology
331 described by Gustard (1983) and WMO (2008). This methodology linearly interpolates between
332 turning points in Q that are defined as local minima within a non-overlapping 5-day window,
333 which are at least 1.11 times smaller than their neighboring minima. Despite its simplicity, this
334 base flow separation method was chosen because it allows for an unambiguous identification of
335 event starting points (Tarasova et al., 2018). We defined the start of an event as the point in time
336 when fast flow increases to at least 2.5 % of base flow and Q has increased by a minimum of 5 %
337 over the previous 5 hours. Events were defined to end when fast flow decreases to less than
338 2.5 % of base flow. The final selection of the event was based on the criterion that the event
339 included a minimum of 20 data points, peak Q reached at least the 5 % percentile of all Q
340 measurements, fast flow contribution at the peak of the event was at least 30 % of total flow and
341 Q decreased at least to one third of its former increase. Events with data gaps larger than 5 hours
342 were discarded from the analysis. These criteria and thresholds were chosen as they allowed for a
343 good balance between the separation of clearly evident events from scatter in Q and the detection

344 of a sufficient number of small-scale events that occurred during low flow seasons (LFSs) to
 345 obtain a fairly equal number of events during all four seasons.

346 Next, we fitted equation (2) to each selected event (Eder et al., 2010; Krueger et al.,
 347 2009; Minaudo et al., 2017) to analyze the event-specific CQ-slope and the hysteresis direction
 348 and extent:

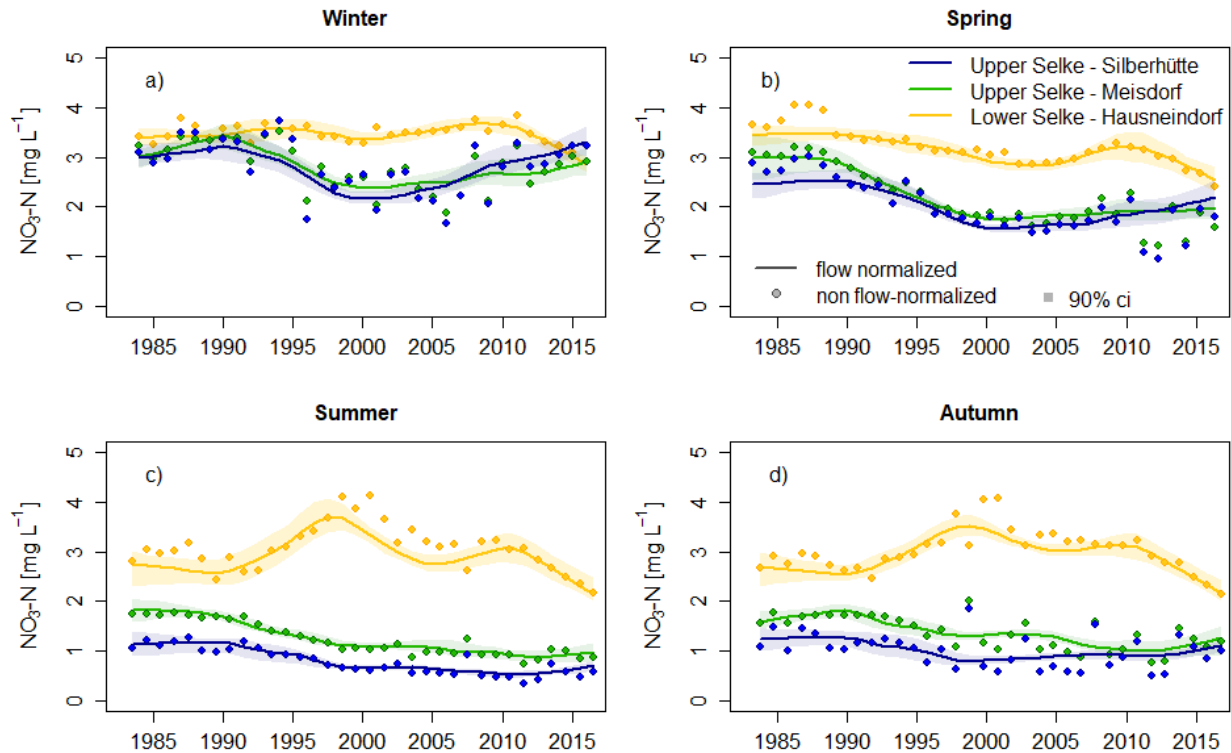
$$349 \quad C = a * Q^b + c * \frac{dq}{dt} \quad (2)$$

350 where a , b and c are parameters that were fitted for each event individually. Parameter a
 351 gives the event-specific intercept and b the CQ-slope, which is comparable to the parameter β_2
 352 from the long-term analysis (eq. 1). Consequently, parameter b was used to differentiate between
 353 chemodynamic-accretion ($b > 0.1$), chemodynamic-dilution ($b < -0.1$) and chemostatic ($-0.1 < b$
 354 < 0.1) nitrate transport during storm events. Parameter c was used to identify the extent and
 355 direction of event-specific hysteresis with $c > 0.1$ indicating clockwise hysteresis, $c < -0.1$
 356 indicating counterclockwise hysteresis and $-0.1 < c < 0.1$ indicating no or complex hysteresis.
 357 Note that dQ/dt was scaled for the individual event to allow a better comparison of c between the
 358 events. The season of an event was defined as the season in which the event starts. To assure the
 359 quality of results, parameters b and c were only used for further analysis if the coefficient of
 360 determination (R^2) for the event-specific fit of eq. 2 was larger than 0.5.

361 **3 Results**

362 **3.1 Seasonal and long-term patterns in nitrate concentrations**

363 Referring to the regular monitoring results between 1983 and 2016, the upper Selke
 364 showed a pronounced seasonality, with lower nitrate concentrations during low flow seasons
 365 (LFSs, summer and autumn) and higher concentrations during high flow seasons (HFSs, winter
 366 and spring), while nitrate concentrations in the lower Selke were more stable between seasons. In
 367 general, the fitted nitrate concentrations increased from the upper to the lower Selke (Fig. 2), but
 368 due to the differences in seasonality, this increase was especially pronounced during LFSs. Here,
 369 FN nitrate concentrations ($\text{NO}_3\text{-N}$) ranged between $0.5 - 1.8 \text{ mg L}^{-1}$ in the upper Selke and
 370 between $2.0 - 3.7 \text{ mg L}^{-1}$ in the lower Selke. During HFSs, the difference between upper and
 371 lower Selke nitrate concentrations was relatively small. Here, FN nitrate concentrations ranged
 372 between $1.6 - 3.4 \text{ mg L}^{-1}$ in the upper Selke and between $2.4 - 3.7 \text{ mg L}^{-1}$ in the lower Selke.
 373 Using WRTDS to fit daily nitrate concentrations resulted in a small bias of 1.7 %, 0.5 % and -
 374 0.5 % for Silberhütte, Meisdorf and Hausneindorf, respectively, with respect to the measured
 375 long-term data.



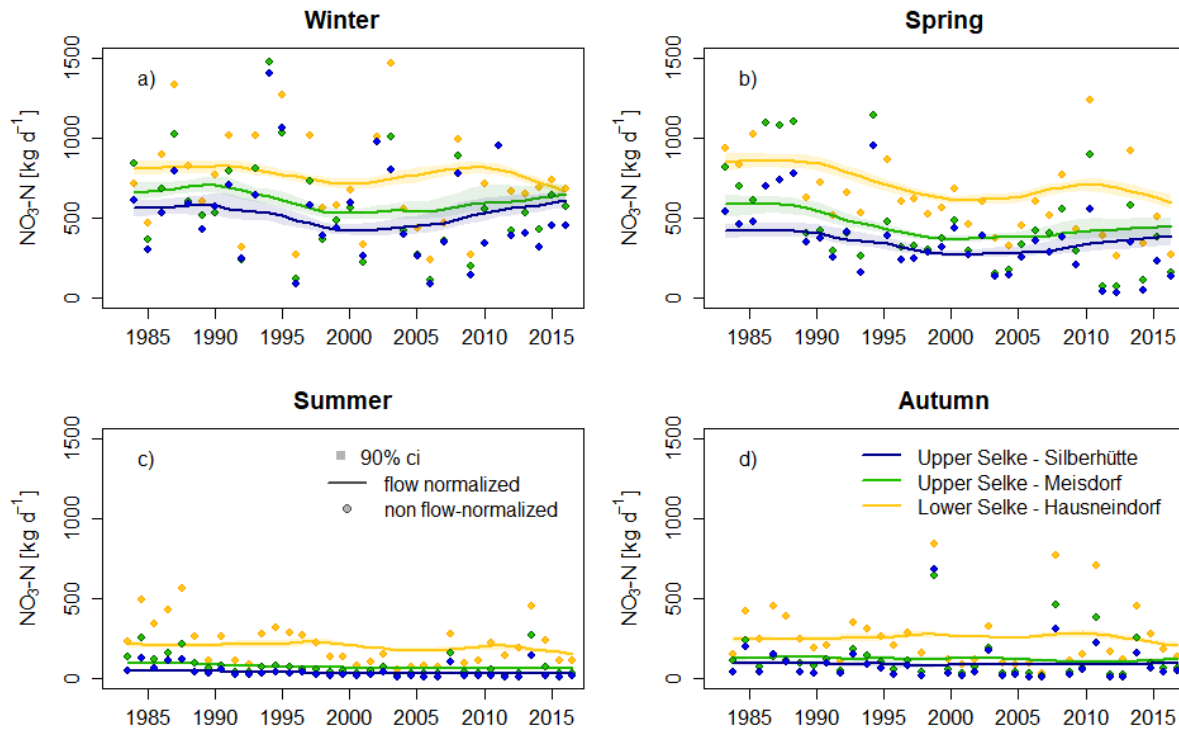
376
 377 **Figure 2.** Long-term trends of annual flow normalized (FN, lines) and annual non-FN (dots)
 378 nitrate concentrations from three nested sub-catchments of the Selke catchment, separated by
 379 season. Uncertainty bands in the sub-catchment specific color indicate the 90% confidence
 380 intervals from bootstrapping FN values.

381 Besides general differences in nitrate concentrations and their different seasonality, long-
 382 term trends also showed a different behavior between upper and lower Selke, again most
 383 pronounced during LFSs. Here, a marginal decrease from 1990 on occurred in the upper Selke,
 384 while in the lower Selke, FN nitrate concentrations increased substantially, with a maximum
 385 value of 3.7 and 3.5 mg L⁻¹ in summer and autumn 1997, respectively. A secondary peak
 386 occurred during 2010 with 3.1 mg L⁻¹ in both seasons (Fig. 2 c,d). In the most recent years (2011
 387 – 2016), nitrate concentrations in the lower Selke during LFSs decreased to an average value of
 388 2.6 mg L⁻¹. During HFSs, nitrate concentrations in the upper Selke decreased more strongly after
 389 1990 but increased again from 2000 on. In the lower Selke, however, only slight temporal
 390 changes occurred during HFSs and the decrease in most recent years - observable during LFSs -
 391 occurred to a lesser extent also during HFSs (Fig. 2 a,b).

392 3.2 Seasonal and long-term behavior of nitrate loads

393 Nitrate loads showed a strong seasonality with highest nitrate loads during HFSs and
 394 lowest during LFSs (Fig. 3). This seasonality was more pronounced in the upper Selke than in
 395 the lower Selke and, consequently, the relative contribution from sub-catchments to nitrate loads
 396 varied seasonally. Overall, highest loads occurred during winter with an average of 515.5 kg d⁻¹
 397 in Silberhütte, 607.8 kg d⁻¹ in Meisdorf and 774.8 kg d⁻¹ in Hausneindorf (average from non-FN
 398 values). If neglecting in-stream losses of nitrate, this implies that the upper Selke transported
 399 78.4 % of the catchment's nitrate loads during winter. Lowest loads occurred during summer

400 with 39.5 kg d^{-1} , 77.4 kg d^{-1} and 207.6 kg d^{-1} for Silberhütte, Meisdorf and Hausneindorf,
 401 respectively. Contrarily to winter, the upper Selke had a much smaller contribution to the
 402 catchments loads of only 37.3 % during summer. On an annual scale, the upper Selke contributed
 403 approximately 64.2 % to the total catchment's nitrate loads. If accounting for the sub-catchment
 404 area, consequently, the average of annual loads were highest in Silberhütte with $8.6 \text{ kg ha}^{-1} \text{ a}^{-1}$,
 405 followed by Meisdorf with $6.3 \text{ kg ha}^{-1} \text{ a}^{-1}$ and smallest in Hausneindorf with $3.9 \text{ kg ha}^{-1} \text{ a}^{-1}$.



406 **Figure 3.** Long-term trends in annual FN nitrate loads (lines) and annual non-flow normalized
 407 nitrate loads (dots) from three nested sub-catchments of the Selke catchment, separated by
 408 season (a-d). Uncertainty bands in the sub-catchment specific color indicate the 90% confidence
 409 intervals from bootstrapping FN values.
 410
 411

412 3.3 Concentration-discharge relationships

413 Long-term CQ-slopes in the upper Selke were positive, indicating chemodynamic nitrate
 414 export with an accretion pattern (Musolff et al., 2017), which was observed in seasonal (Fig. 4)
 415 as well as in annual CQ-slopes (Fig. S2 c). The only exception was Meisdorf during LFSs
 416 between 1983 and 1990, where nitrate export was chemostatic with a CQ-slope close to zero
 417 (Fig. 4 c,d). CQ-slopes in Silberhütte were higher than the ones in Meisdorf, except for HFSs
 418 from 2010 on, where CQ-slopes were both around 0.45 (Fig. 4 a,b). During LFSs, CQ-slopes in
 419 the upper Selke peaked in 1999 and, following a minimum around 2005, leveled out afterwards.
 420 Uncertainty assessed via bootstrapping was highest for LFSs, but the generally positive CQ-
 421 slopes from 1990 on were still evident (Fig. 4 c,d).

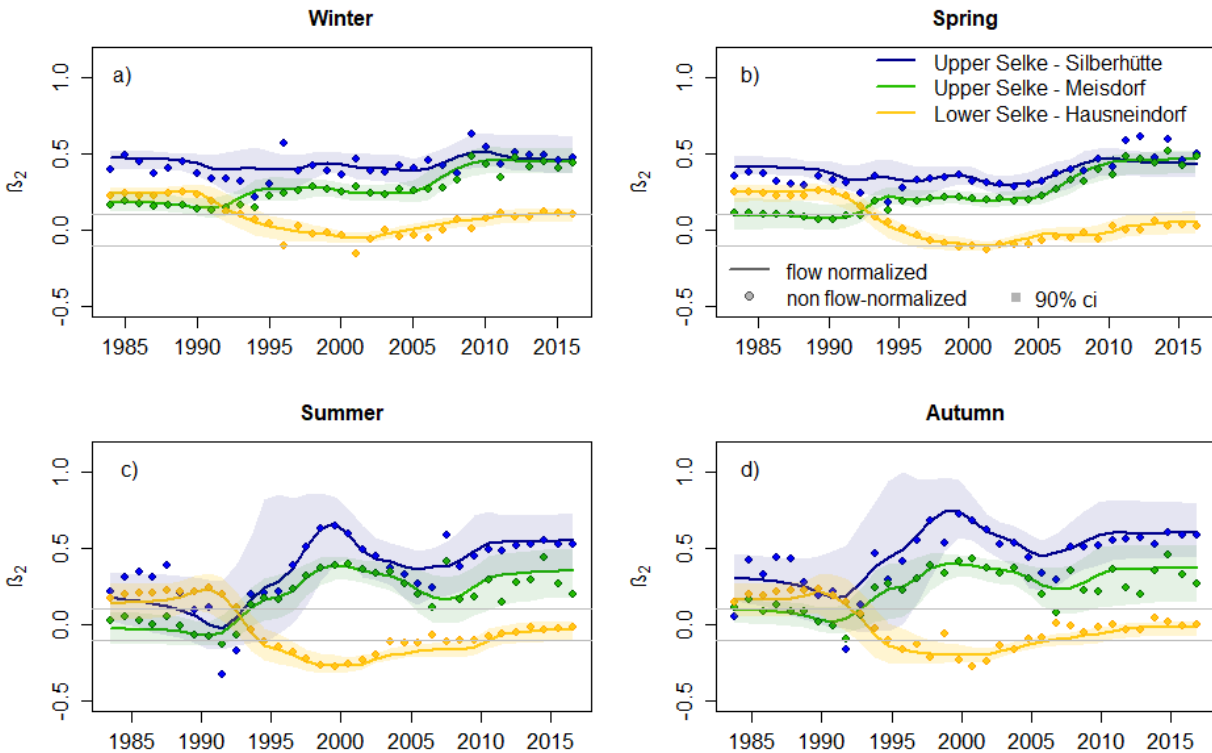
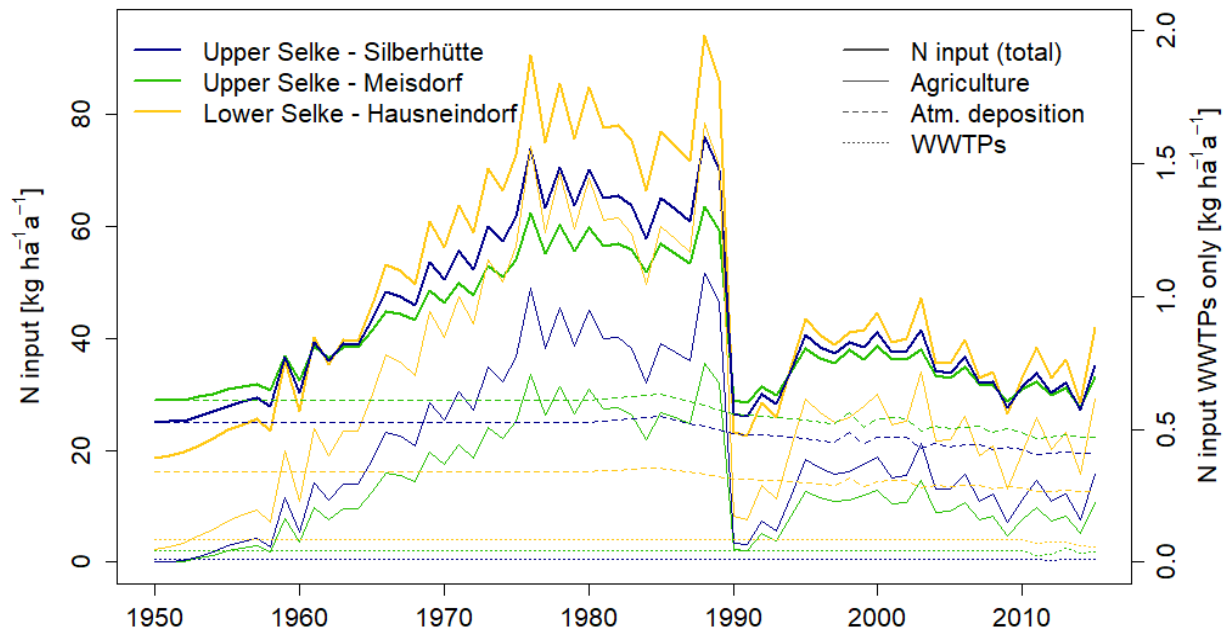


Figure 4. Long-term trends of the fitted parameter β_2 , indicating the annual flow normalized (FN) and annual non-FN $\ln(\text{concentration})-\ln(\text{discharge})$ relationship (CQ-slope) from three nested sub-catchments in the Selke catchment, separated for each season. Uncertainty bands in the sub-catchment specific color indicate the 90% confidence intervals from bootstrapping FN values.

In contrast to the upper Selke, the export regime in the lower Selke changed significantly over time (Fig. 4, Fig. S2). CQ-slopes in the lower Selke were positive between 1983 and 1990 for all seasons, which indicates chemodynamic nitrate transport with accretion patterns. After 1990, CQ-slopes decreased towards values around zero during HFSs (Fig. 4 a,b), which indicates chemostatic transport, and towards negative CQ-slopes during LFSs (Fig. 4 c,d), which indicates chemodynamic nitrate export with a dilution pattern. From around 2010 on, nitrate transport in the lower Selke was chemostatic during all seasons with a tendency to slightly higher CQ-slopes during HFSs compared to LFSs.

3.4 Nitrogen budget

Since the start of the time series in 1950, N input strongly increased until 1976 and fluctuated between 1976 and 1989 around an average N input of $57.3 \text{ kg ha}^{-1} \text{ a}^{-1}$ in the upper Selke and $79.4 \text{ kg ha}^{-1} \text{ a}^{-1}$ in the lower Selke. Maximum N input was reached in the year 1988. In 1990, after the reunification of Germany and the associated break down of the intensive agriculture in East Germany (Gross, 1996), N input decreased drastically within one year and then stabilized again on a lower level around $33.9 \pm 3.3 \text{ kg ha}^{-1} \text{ a}^{-1}$ (upper Selke) and $37.7 \pm 5.2 \text{ kg ha}^{-1} \text{ a}^{-1}$ (lower Selke) from 1995 onwards (Fig. 5, Table 1).



446
447
448
449
450
451

Figure 5. Total N input per hectare and year for all three nested sub-catchments of the Selke catchment and N input divided into its components i) from agricultural areas, ii) atmospheric deposition and biological fixation on non-agricultural areas, and iii) outflow from wastewater treatment plants (WWTPs, second y-axis).

452 Annual N input per hectare (ha) was generally lower for the upper Selke (representing the
453 catchment area draining to the gauge at Meisdorf) than for the lower Selke (representing the
454 entire catchment area draining to the gauge at Hausneindorf; Fig. 5; Table 1). The only
455 exceptions were found during years, when the total N input was especially low (e.g. 1990/91). In
456 these years, the scenario reversed with highest N input in the upper Selke and lowest N input in
457 the lower Selke, due to a relatively high atmospheric N deposition over the Harz Mountains and
458 biological N fixation in the forests (Fig. 5, Table 1). Between 1983 and 2015, approximately one
459 third (34.5 %) of N input stemmed from the upper Selke and most of this from the upstream area
460 draining to the gauge at Silberhütte (Table 1). N surplus from agriculture in this period was
461 around 33 % and 68 % of the total N input for the upper and lower Selke, respectively. The
462 remaining part mainly stemmed from natural areas (mainly forests and grasslands), while the
463 contribution from WWTPs was small. If assuming constant N input from WWTPs over the year,
464 they contributed on average 0.8 % - 1.6 % to exported annual nitrate loads in the upper Selke and
465 2.4 % - 3.6 % in the lower Selke (assuming no or a complete nitrification of wastewater-born
466 ammonium). During LFSs, the contribution from WWTPs to nitrate export was on average
467 3.4 % - 7.4 % and 6.2 % - 9.5 % for the upper and lower Selke, respectively.

468 3.5 Nitrate retention and transit time distributions

469 Modes and μ -values of the lognormal TTDs fitted as a transfer function between annual
470 N input and annual FN nitrate concentrations show that TTs in the upper Selke were
471 considerably shorter than those in the lower Selke (Table 1). The convolution model was
472 accurate for the upper Selke at Meisdorf ($R^2 = 0.92$) and acceptable for Silberhütte ($R^2 = 0.57$) as
473 well as for the lower Selke ($R^2 = 0.40$; Table 1).

474 TTD derived conservative N export over the period from 1983 to 2015 was higher than
 475 N input for this period (Table 1), because it integrated parts of the high N input from before
 476 1983. We refer to the TTD derived conservative N export that was not exported in form of
 477 measured annual nitrate loads as the *missing N* (Van Meter et al., 2016; Table 1), which is either
 478 still in the catchments as legacy or removed via denitrification. All sub-catchments of the Selke
 479 catchment showed a considerably percentage of missing N (80 – 92%). This number is smallest
 480 for the upper Selke, especially for the upstream area draining to the gauge at Silberhütte, and
 481 largest for the lower Selke, with 10.8-11.5 kg ha⁻¹ a⁻¹ more N being missing than in the upper
 482 Selke.

483
 484 **Table 1.** Transit time distributions (TTDs) and the balance between nitrogen (N) input and its
 485 riverine export as nitrate loads

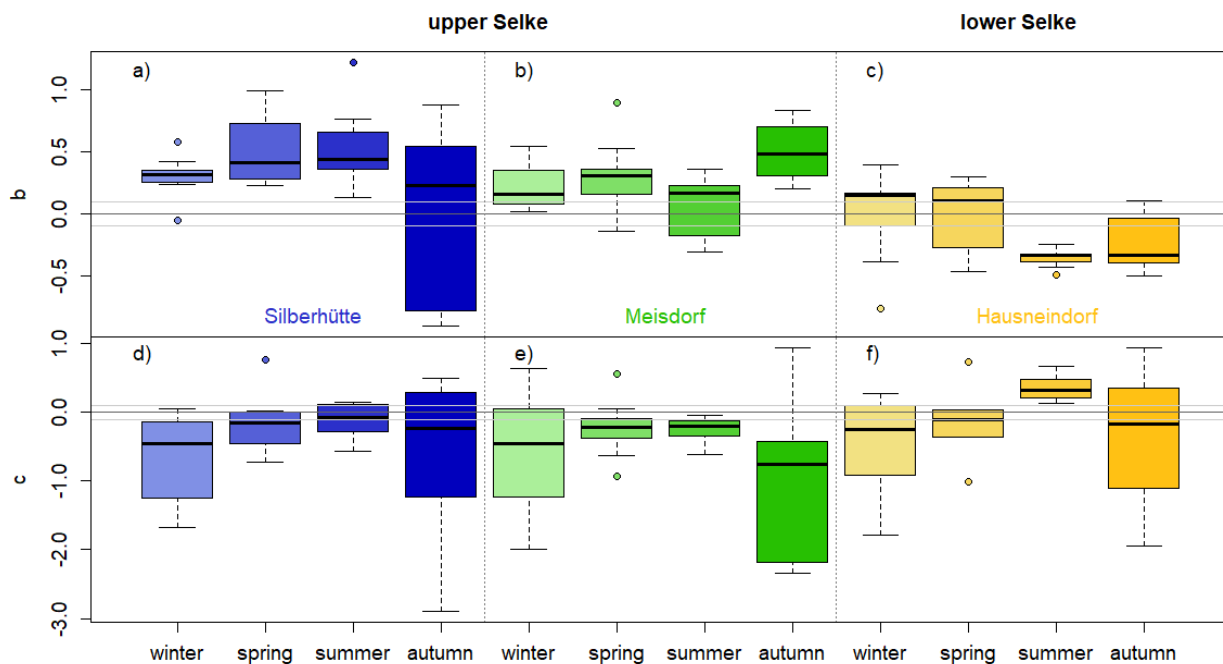
		unit	upper Selke		lower Selke
			Silberhütte	Meisdorf	Hausneindorf
TTDs	μ	[a]	2.12	1.59	2.91
	σ	[a]	1.15	1.10	0.73
	R ²	[-]	0.57	0.92	0.40
	Mode (year of peak travel time)	[a]	3	3	12
N input vs. export (1983 – 2015)	Cumulative N input	[t]	14078.7	23195.4	67146.9
	N export _{conv} (conservative)	[kg ha ⁻¹ a ⁻¹]	44.3	41.2	50.3
	Cumulative N export _{conv} (conservative)	[t]	15352.9	25045.3	75753.0
	Cumulative N export, (measured)	[t]	3052.1	3912.0	6094.3
	Missing N (conservative - measured)	[kg ha ⁻¹ a ⁻¹]	35.5	34.8	46.3
		[t]	12300.7	21133.3	69658.6
[%]		80.1	84.4	92.0	

486 *Note.* TTDs follow a log-normal distribution with fitted parameters μ and σ and the R² as the
 487 coefficient of determination. Conservative N export is the N input convolved with TTDs as
 488 indicated by subscript *conv*. *Missing N* refers to the difference between conservative N export
 489 and measured N export in form of riverine nitrate loads.

490 3.6 Storm events

491 We identified a total of 200 storm events, with 59 for Silberhütte (over the period from
 492 2013 to 2016), 72 for Meisdorf and 69 for Hausneindorf (both over a period from 2010 to 2016).
 493 From all these events, 56 % could be described adequately with the empirical formula defining
 494 the hysteresis loop (eq. 2) with R² > 0.5. This corresponds to 40 events in Silberhütte, 44 in
 495 Meisdorf and 29 in Hausneindorf, with at least seven events per season and gauge. Fitted
 496 parameters *b* and *c* for event-specific CQ-slopes and hysteresis behavior of these events are
 497 displayed in Fig. 6. Upper Selke CQ-slopes were dominantly positive, indicating chemodynamic
 498 nitrate export during storm events with an accretion pattern (Fig. 6 a,b). Some exceptions were

499 found during autumn in Silberhütte, where some small events during November showed negative
 500 CQ-slopes and caused a large variability in CQ-slopes during this season (Table S1) and during
 501 summer in Meisdorf. Event-specific hysteresis in the upper Selke was dominantly
 502 counterclockwise, indicated by the negative parameter c (Fig. 6 d,e). In contrast to the upper
 503 Selke, event-specific CQ-slopes in the lower Selke were negative during LFSs, indicating
 504 chemodynamic nitrate transport with a dilution pattern (Fig. 6 c). During HFSs however, event
 505 specific CQ-slopes were dominantly positive, indicating an accretion pattern, similar to the upper
 506 Selke. Hysteresis during summer was clockwise, and dominantly counterclockwise during all
 507 other seasons, again similar to the upper Selke. For all three sub-catchments, variability in
 508 hysteresis behaviour was most pronounced during autumn. If looking at all identified events –
 509 regardless of their R^2 (Fig. S3) – the described patterns in CQ-slopes and hysteresis stayed
 510 evident, with the only exception that CQ-slopes in the lower Selke during spring were
 511 dominantly around zero or negative.



512 **Figure 6.** Boxplots of the event-specific fitted parameters b (CQ-slope) and c (hysteresis) in eq.
 513 2 with $R^2 > 0.5$. Parameters were separated by seasons and gauging stations within the Selke
 514 catchment, displayed from upstream (left) to downstream (right).
 515
 516
 517

518 4 Discussion

519 4.1 Long-term trends in nitrate export

520 To understand how nested sub-catchments affect the response of nitrate export to changes
 521 in N-surplus, the drastic N input change in 1990 together with the nested catchment structure
 522 gave an ideal setting to analyze the long-term response from different sub-catchments (Ehrhardt
 523 et al., 2019). The question of how long these input changes need to propagate through the
 524 catchment subsurface until they are measurable in the stream, can mainly be answered by the
 525 sub-catchment specific nitrate TTDs, which showed a clear difference between the upper and the

526 lower Selke. While in the upper Selke, the TTDs showed a peak after three years indicating a
527 dominance of short transit times, the TTD in the lower Selke showed a peak after 12 years and
528 therefore had a considerably longer tailing (Table 1). Consequently, N input in the upper Selke is
529 transported rapidly to the stream network and the response of instream nitrate concentrations to
530 changes in N input becomes visible almost immediately, while in the lower Selke, N input is
531 transported far more slowly and the response of nitrate concentrations to changes in N input is
532 delayed by more than a decade. Long-term persistence of nitrate pollution is, therefore, rather an
533 issue in the agriculturally dominated lower Selke than in the upper Selke.

534 The sub-catchment specific differences in TTDs helped to explain the different long-term
535 trends in nitrate concentrations, loads and CQ-slopes (Fig. 2 and 4). In the upper Selke, short TTs
536 mainly explain the immediate decrease of nitrate concentrations and loads after 1990 as a
537 response to the drastic N input decrease, which is supported by a study from J. Yang et al. (2018)
538 who found short TTs of around 79 days for a small headwater catchment in the upper Selke (1.44
539 km²) and by other studies that report short TTs in typical upland catchments with a responsive
540 hydrological regime (e.g. Hrachowitz et al., 2009; Soulsby et al., 2015). The increase in nitrate
541 concentrations and loads from 2000 on, however, cannot be explained by TTDs and N input;
542 instead, it coincided with an increase in CQ-slopes (Fig. 4), reflecting that nitrate concentrations
543 increased during HFSs but stayed similar during LFSs (Fig. 2). One possible explanation is that
544 local changes in agricultural practices, forest management or land use arrangement, which were
545 not accounted for in the county-level N input data, might have changed the amount and
546 connectivity of nitrate sources to streams and the consequent degree of nitrate mobilization
547 during high flow conditions.

548 In contrast to the upper Selke, long TTs in the lower Selke led to a delayed reaction of
549 instream nitrate concentrations to changes in N input, such as the drastic decrease in 1990.
550 Directly after this input decrease, nitrate concentrations during LFSs contrarily increased in the
551 lower Selke (Fig. 2 c,d). Most likely, this increase reflects the delayed response to the peak in N
552 input from before 1990 (Fig. 5), while the decrease in N input in 1990 became measurable in
553 riverine nitrate concentrations only about a decade later (Figs. 2 and 3). However, the two
554 emerging peaks in nitrate concentrations during LFSs (1997 and 2000) in the lower Selke and the
555 striking decrease after 2010 during all seasons (Fig. 2) cannot be explained by transit times
556 alone. Agricultural and more densely populated catchments are typically exposed to a large
557 number of different nitrate sources and anthropogenic impacts (Caraco & Cole, 1999; Silva et
558 al., 2002). In the lower Selke, the starting operation of WWTPs around 1996/1997 and the
559 activities around the mining pit close to the catchment outlet are likely drivers for individual
560 peaks in the analyzed long-term trends. Furthermore, the water that was added to the Selke River
561 since 2009 to keep the water level in the mining lake constant, likely caused a dilution of riverine
562 nitrate concentrations and might have been one reason for the decrease of nitrate concentrations
563 in recent years (Fig. 2, Fig. S4). Another possible reason might be a decline in groundwater
564 recharge due to climate change that caused a lower mobilization of nitrate from the groundwater
565 to the stream network. Hence, although the decrease in nitrate concentrations in the lower Selke
566 is generally a good sign for water quality, the driving forces are related to considerable
567 uncertainty. Nitrate concentrations might have decreased due to a delayed reaction from the
568 decrease in N input 1990, due to a decline in groundwater recharge or due to the dilution with
569 water from the flooded mining pit with lower nitrate concentrations. We assume that a
570 combination of all these processes was responsible for the observed concentration declines.

571 CQ-slopes in the lower Selke changed from i) an accretion pattern before 1990 to ii)
572 dilution in LFSs and chemostasis in HFSs and finally towards iii) chemostatic nitrate export
573 during all seasons in recent years (Fig. 4). A very similar dynamic of CQ-slopes was reported by
574 Ehrhardt et al. (2019) for a nearby mesoscale catchment. They explained this by the vertical
575 stratification of nitrate storage in the subsurface as a consequence of the downward transport of
576 nitrate with time (Dupas et al., 2016) and different active flow paths during HFSs and LFSs.
577 During LFSs, Q is dominated by base flow that originates from deeper groundwater, while
578 during HFSs, shallower subsurface flow paths are activated that access a younger fraction of
579 groundwater (Ehrhardt et al., 2019; Musolff et al., 2016). As N input gradually increased until
580 1976, deeper groundwater in the lower Selke in the first years of our time series still showed
581 lower nitrate concentrations than shallow groundwater. Consequently, nitrate concentrations
582 during low flow conditions were lower than concentrations during high flow, leading to the
583 observed accretion pattern. After the German reunification in 1990, N input drastically decreased
584 leading to a decrease of nitrate concentrations in shallow groundwater and higher concentrations
585 in deeper groundwater due to the downward percolation of the high N inputs from before 1990
586 (Fig. 5). Consequently, nitrate concentrations in the lower Selke were higher during low flow
587 conditions than during high flow conditions, leading to the observed dilution pattern. Another
588 reasonable explanation for the dilution pattern is the impact from upper Selke nitrate export. Due
589 to the shorter TTs in the upper Selke, long-term trends in riverine nitrate concentrations showed
590 an immediate decrease after 1990, while concentrations still increased in the lower Selke. This
591 diverging long-term trends were especially pronounced during LFSs (Fig. 2 c,d). Lower nitrate
592 concentrations from the upper Selke during LFSs could have, therefore, diluted the higher nitrate
593 concentrations downstream, leading to the observed dilution pattern in CQ-slopes in the lower
594 Selke (Figs. 4 c,d and S2 c). Most plausibly, a mixture of both vertical layering of groundwater
595 nitrate concentrations and the impact of the upper Selke led to the observed dilution pattern. In
596 recent years, chemostatic nitrate export during all seasons developed in the lower Selke, likely
597 due to a mixture of both vertical equilibration of groundwater nitrate concentrations after a
598 prolonged period of stable N inputs (Fig. 5; Dupas et al., 2016; Ehrhardt et al., 2019) and a less
599 pronounced dilution effect from the upper Selke due to converging nitrate concentration levels
600 between the sub-catchments (Fig. 2).

601 Similar to Ehrhardt et al. (2019), we could show that CQ-relationships transitionally shift
602 with changes in N input and further that these changes can be different between seasons. Thus,
603 chemostatic nitrate export is not exclusively an indication for intensive agriculture but also for
604 homogeneously distributed N stores, both vertically in the subsurface and between different sub-
605 catchments. In fact, chemodynamic export at the catchment outlet can also indicate ‘not
606 equilibrated systems’, where changes in N input have not yet propagated through the whole
607 system, causing a vertical layering of nitrate concentrations in the subsurface and/or diverging
608 nitrate concentration between sub-catchments due to different sub-catchment specific TTDs.
609 Defining one unique CQ-slope for nitrate concentrations at the catchment outlet across longer
610 time series and seasons can be misleading as may it integrates input and mobilization patterns as
611 well as transport times that are not necessarily the same over space and time (Fig. S5). For
612 example a temporal transition from accretion patterns towards dilution - as observed in the lower
613 Selke during LFSs from 1990 to 2000 - might be interpreted as constantly chemostatic if not
614 accounting for these transitional changes and for seasonal differences.

615 4.2 N legacies and potential denitrification

616 Measured nitrate export accounted for approximately 15.4 % and 8.0 % of the TTD
617 derived conservative estimate of N export for the upper and lower Selke, respectively. This
618 translates into $34.8 \text{ kg N ha}^{-1} \text{ a}^{-1}$ and $46.3 \text{ kg N ha}^{-1} \text{ a}^{-1}$ missing N (Table 1) and is a first evidence
619 for considerable N retention in both sub-catchments, especially in the lower Selke. Fast TTs in
620 the upper Selke indicate a dominance of biogeochemical legacies and only a minor impact of
621 hydrological legacies. CQ-slopes and the pronounced seasonality, furthermore, indicate that N
622 sources are either stored in the shallower zones of the sub-surface or in the more distant zones to
623 the stream network, which could both be partially activated during high flow conditions such as
624 storm events during winter. This explanation is supported by J. Yang et al. (2018), who proposed
625 that an expansion of Q generating zones during high flow conditions in a small headwater
626 catchment in the upper Selke enables the mobilization of additional N sources. In contrast in the
627 lower Selke, long TTs and the shifts in CQ-relationships indicate a dominance of hydrological
628 legacies over biogeochemical ones, as nitrate export patterns are driven by the seasonal
629 activation of different N source zones with different ages, as discussed above (Ehrhardt et al.,
630 2019).

631 Denitrification is the only process leading to permanent nitrate removal from the
632 catchment. It accounts for a part of the missing N and prevents it from being stored in the
633 catchment (Seitzinger et al., 2006). Kuhr et al. (2014) simulated average denitrification rates for
634 soils in Saxony-Anhalt using the process-based DENUZ transport model (Köhne and Wendland,
635 1992; Kunkel and Wendland, 2006) and showed that denitrification rates in the unsaturated zone
636 in and around the Selke catchment are low to very low ($9 - 13 \text{ kg ha}^{-1} \text{ a}^{-1}$), which is considerably
637 lower than the rates of missing N for the Selke catchment mentioned above (Table 1). Even
638 assuming the upper range denitrification rate, missing N would still be $>20 \text{ kg N ha}^{-1} \text{ a}^{-1}$ in the
639 upper and $>30 \text{ kg N ha}^{-1} \text{ a}^{-1}$ in the lower Selke.

640 The potential for denitrification in the groundwater is largely depleted in Saxony Anhalt,
641 according to a recent study from Hannappel et al. (2018). From the seven observation wells
642 within the Selke catchment, only one showed evidence for ongoing denitrification, which was
643 located in the upper Selke. Hence, denitrification in the groundwater likely removed a part of N
644 input in the upper Selke. However, from all observation wells in Saxony-Anhalt located on a
645 similar geologic setting as the upper Selke (Palaeozoic), less than 5% showed evidence for
646 ongoing denitrification. This is a warning sign for the upper Selke, indicating that essential
647 electron donors such as pyrite for autolithotrophic denitrification have been largely consumed or
648 might get depleted in the near future. In the lower Selke, none of the observation wells showed a
649 potential for denitrification in groundwater (Hannappel et al., 2018). We, therefore, argue that
650 denitrification in groundwater played only a minor role for the fate of N input in the lower Selke,
651 which is in line with findings from Ehrhardt et al. (2019) in a nearby mesoscale catchment.
652 Nevertheless, there is evidence for significant denitrification in the riparian zones, especially
653 during LFSs. Recent studies by Lutz et al. (2020) and Trauth et al. (2018) reported a removal by
654 riparian denitrification of up to 12 % of nitrate from groundwater entering the Selke River along
655 a 2 km section downstream of Meisdorf. Additionally, a stable isotope study of Müller et al.
656 (2015) in the Bode catchment, which includes the Selke catchment, found evidence for
657 significant denitrification in the stream beds during LFSs while denitrification in the
658 groundwater was not evident, in line with Hannappel et al. (2018). The studies agree that riparian
659 zone and stream bed denitrification are more likely to occur in the downstream part of the river

660 where flow velocities are reduced, which suggests that this type of denitrification might be an
661 important process for the lower but not evidently for the upper Selke.

662 Assimilatory uptake in the stream is another important process for nitrate export
663 dynamics, which could, according to Rode et al. (2016), have removed around 5 % of nitrate in
664 the upper Selke and 13 % in the lower Selke. Nevertheless, the permanent removal via
665 denitrification accounts for only a small percentage of assimilatory uptake. Hence, we suggest
666 that assimilatory uptake does only account for a small percentage of the missing N. Moreover,
667 following the argument of Ehrhardt et al. (2019), the change in seasonal patterns in the lower
668 Selke and the high nitrate concentrations in LFSs around 1997 (Fig. 2 c,d) indicate that
669 assimilatory uptake was not a key process causing the observed nitrate export patterns at longer
670 time scales, as this would imply a more steady seasonality.

671 In summary, a large portion of N was not exported from the Selke River and is therefore
672 missing. It is unlikely that denitrification alone is responsible for all missing N, which means that
673 parts of it were stored as legacies. We argue that biogeochemical legacies dominate in the upper
674 Selke, while long TTs and deeper aquifers lead to a dominance of hydrological legacies in the
675 lower Selke. As N input and the percentage of missing N in the lower Selke was higher,
676 extensive N legacies and especially long-term nitrate pollution are more of an issue in the
677 agriculturally dominated lowland parts of the catchment than in the mountainous upstream part.
678 Groundwater dominated catchments like the lower Selke are generally more prone to
679 hydrological legacies (Van Meter & Basu, 2017). As these (sub-)catchments are typically
680 associated with agricultural land use, they are most prone to developing nitrate legacies.

681 4.3 Seasonality in nitrate export

682 The contribution from different sub-catchments to nitrate export in the Selke catchment
683 was highly seasonal, with significant differences between HFSs and LFSs. While the upper Selke
684 dominated nitrate export during HFSs, the lower Selke dominated during LFSs. This seasonal
685 shift in the dominant sub-catchment for nitrate export was driven by the seasonally different
686 dynamics of mobilization and transport in the different sub-catchments.

687 Nitrate concentrations in the upper Selke showed a pronounced seasonality with high
688 concentrations during HFSs and low concentrations during LFSs, a dynamic that was reflected
689 also by positive the CQ-slope, indicating a chemodynamic-accretion pattern (Fig. 4). This
690 accretion pattern can be explained by the activation of additional N sources with efficient
691 transport to the stream during wet conditions (J. Yang et al., 2018). In contrast to chemostatic
692 patterns, N sources are not uniformly distributed but rather distinct sources become activated
693 during certain flow conditions. Therefore, accretion patterns hint at patchy N sources and
694 spatially limited N legacies. This might be a common situation in mountainous upstream
695 catchments that include only patches of agriculture or other relevant N sources. The consequent
696 increase in nitrate concentrations during high flows can cause high nitrate loads, as observed in
697 the upper Selke. Although it is known that upstream catchments can have an important role for
698 nutrient transport (Alexander et al., 2007; Goodridge & Melack, 2012), the contribution from the
699 upper Selke to 78.4 % of overall nitrate loads during winter and 64 % on the annual scale was
700 unexpectedly high, given the fact that the upper Selke comprises only 17 % of the catchment's
701 agricultural area and contributed on average only 37 % of total N input. We explain this
702 disproportional contribution to nitrate loads by the high nitrate concentrations during HFSs

703 (reflected by the described accretion pattern) together with a disproportional contribution to Q,
704 which is typical for upstream catchments (Alexander et al., 2007; Dupas et al., 2019).

705 Nitrate concentrations in the lower Selke generally showed a less pronounced seasonality
706 compared to the upper Selke, especially since 2010, when nitrate export became chemostatic
707 during all seasons (Fig. 4). Chemostatic export was often found for catchments like the lower
708 Selke that are dominated by agricultural land use, indicating a considerable amount of nitrate
709 legacy stores (Basu et al., 2010, 2011) and a prolonged period of relatively stable N inputs
710 (Ehrhardt et al., 2019). Due to the decreasing contribution from the upper Selke during LFSs and
711 base flow conditions, the relatively constant nitrate input (around 3.1 mg L^{-1}) in the lower Selke
712 kept nitrate concentrations high during these periods and consequently dominated nitrate export
713 under dry conditions when surface waters are subject to an increased risk of eutrophication and a
714 consequent loss of aquatic biodiversity (Whitehead et al., 2009). Another factor that could have
715 caused high or non-decreasing nitrate concentrations during LFSs, is the constant contribution
716 from WWTPs that have a relatively higher impact when stream Q is low. However, their overall
717 contribution to nitrate export in the lower Selke was low even during LFSs (6.2 - 9.4 %) and the
718 dilution pattern during events indicates no significant impact from rainwater overflow basins.
719 Outflow from WWTPs were therefore certainly not the dominant driving force for elevated
720 nitrate concentrations during LFSs.

721 In conclusion, the pronounced seasonality in the upper Selke leads to a dominance of
722 nitrate export during HFSs and a disproportional contribution to annual nitrate loads. During
723 LFSs, the contribution to nitrate export from the upper Selke is small and consequently the
724 relatively constant nitrate export from the lower Selke dominates. The integrated signal of nitrate
725 export patterns, measured at the catchment outlet, is not a constant mixture of sub-catchment
726 specific signals but reflects a seasonal dominance of different sub-catchments. These results
727 emphasize the importance of analyzing seasonal dynamics in different parts of larger catchments
728 in order to identify the patterns of most dominant N sources at different times of the year (under
729 different hydrological conditions) and thus the temporal interplay between different high-risk
730 zones for N pollution.

731 4.4 Event dynamics and their seasonality

732 To examine the integrated signal of nitrate export across time scales, we analysed not
733 only long-term trends and seasonal patterns, but also the CQ-slopes and hysteresis behaviour
734 during single events. Because high-frequency data for event analysis were available between
735 2010 and 2016, we could directly compare long-term trends and event dynamics during this
736 common period. Event-specific as well as long-term CQ-slopes in the upper Selke were
737 dominantly positive, indicating chemodynamic export with an accretion pattern that is time-scale
738 independent (Fig 6 a,b). Large storm events, therefore, can mobilize and transport large amounts
739 of nitrate and contribute disproportionately to annual nitrate loads. The counterclockwise
740 hysteresis found for most events (Fig. 6 d,e) indicates that N sources are mobilized with a delay
741 to Q, which can be explained by distant N sources and higher nitrate concentrations in riparian
742 floodplain aquifers that dominate the falling limb of event-Q (Rose et al. 2018; Sawyer et al.
743 2014).

744 In the lower Selke, long-term CQ-slopes between 2010 and 2016 showed a chemostatic
745 pattern, while event specific CQ-slopes were more dynamic (Fig. 4; Fig. 6 c). The event-specific
746 dilution patterns (negative CQ-slopes) in LFSs in the lower Selke can be explained by lower

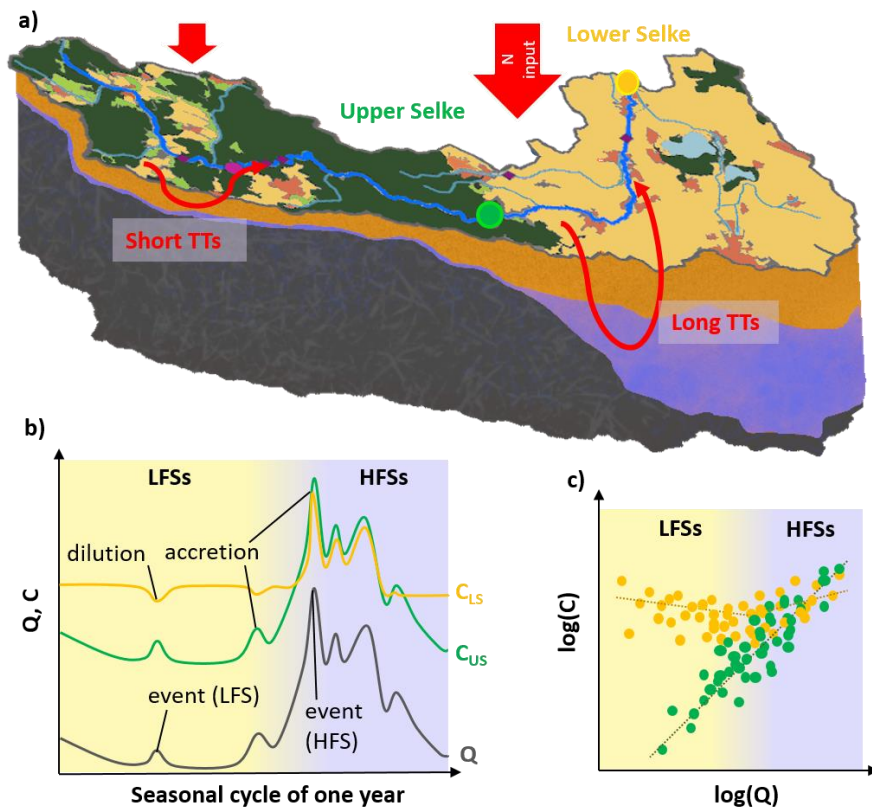
747 nitrate concentrations from the upper Selke (Fig. 2 c,d) that diluted lower Selke nitrate
748 concentrations or by a direct dilution from shallow flow paths that were activated during events
749 and diluted the more highly concentrated base flow. During HFSs, event specific CQ-slopes in
750 the lower Selke became dominantly positive (Fig. 6 c), indicating a chemodynamic export with
751 an accretion pattern same as in the upper Selke. It is also during HFSs that- in recent years -
752 nitrate concentrations from the upper Selke were similarly high than nitrate concentrations in the
753 lower Selke (Fig. 2 a,b). It is, therefore, reasonable to assume that higher nitrate concentrations
754 from the upper Selke during storm events caused an increase in concentrations also in the lower
755 Selke and led to the described accretion pattern during winter-events. The observed
756 counterclockwise hysteresis during winter confirms this assumption, because it was also
757 observed in the upper Selke and indicates more distant nitrate sources (Musolff et al., 2017)
758 which, in this case, might represent the impact from the upper Selke. For both dilution from
759 spring to autumn and accretion during winter, the event dynamics in the lower Selke are
760 considerably influenced by the upper Selke nitrate export.

761 Event specific CQ-slopes estimated at the catchment outlet (lower Selke) are in
762 accordance with findings from Bowes et al. (2015), who reported a dominance of dilution
763 patterns during storm events at the outlet of a mesoscale catchment that integrates different types
764 of land use (39 % arable, 27 % grassland and 23 % woodland). Similarly to our study, the only
765 accretion pattern was observed during winter. Bowes et al. (2015) related this accretion pattern to
766 an additional mobilization of distant agricultural N-sources, which are comparable to our
767 findings with respect to mobilization from the upper Selke. Furthermore, they argued that diffuse
768 N-sources become depleted throughout large storm events in winter and spring, which might also
769 apply to a lesser extend in the upper Selke catchment and explain its lower export of nitrate
770 during spring compared to winter (Fig. 2, 4). Moreover, Dupas et al. (2016) found a similar
771 dilution pattern during most storm events at the outlet of a mesoscale catchment in Thuringia
772 (Saxony-Anhalt, Germany), while long-term trends increasingly showed chemostasis, as
773 observed in the lower Selke. These comparisons show that nitrate export patterns observed at the
774 Selke catchment are not an isolated phenomenon. Taking advantage of the nested catchment
775 study design in the Selke catchment that allowed to identify sub-catchment specific
776 contributions, we suggest that the contrast between long-term and event specific CQ-slopes in
777 the lower Selke reflects the upstream sub-catchment export patterns and therefore serves as an
778 indicator to disentangle sub-catchment specific contributions to nitrate export and its dynamics.

779 4.5 Conceptual framework and implications for management

780 A key objective of this study was to analyze how the integrated response of nitrate
781 concentrations, loads and CQ-relationships at the outlet of a mesoscale catchment is composed
782 by the specific contributions from its nested sub-catchments. While upstream sub-catchments are
783 known to have a disproportional impact on nutrient transport (e.g. Alexander et al., 2007; Dodds
784 & Oakes, 2008; Goodridge & Melack, 2012), agricultural areas, which are more likely to occur
785 in downstream lowlands, are known to be a major source for nitrate pollution (e.g. Padilla et al.,
786 2018; Strebel et al., 1989). The available long-term and high-frequency data for 3 nested
787 catchments within the Selke catchment allowed to disentangle these contrasting drivers of nitrate
788 export and allowed for a detailed analysis of the relative impact of more mountainous upstream
789 sub-catchments (upper Selke) versus more intensively cultivated downstream lowlands (lower
790 Selke) across time scales. The general findings are summarized in Fig. 7, illustrating that TTs for
791 nitrate in the upper Selke were relatively short (Fig. 7 a) and transport patterns were quite

792 dynamic with nitrate concentration increasing with Q (Fig. 7 b,c). These dynamics led to
 793 relatively short-term impacts of temporally elevated nitrate concentrations during HFSs and
 794 events and a disproportional contribution to annual nitrate loads. On the contrary, the lower
 795 Selke showed long TTs (Fig. 7 a) and a less dynamic export behaviour with relatively constant
 796 nitrate concentrations (Fig. 7 b,c). Due to the long TTs, the imbalance between TTD derived
 797 conservative N export and measured N export and the low potential for denitrification, legacy
 798 stores in the downstream part are expected to be significant. Consequently, nitrate pollution in
 799 the lower Selke is a rather long-term and persistent problem that likely dominate nitrate exports
 800 during LFSs and base flow conditions for years to come. This differentiation between a more
 801 mountainous upper part of a catchment and an agriculturally dominated lowland part is not
 802 exclusive to the Selke, but very common for many mesoscale catchments in temperate climates
 803 (e.g. Krause et al., 2006; Montzka et al., 2008). Hence our findings have far reaching
 804 consequences for the management of nitrate pollution in such catchments.



805
 806 **Figure 7.** Conceptual framework explaining the sub-catchment specific contribution from the
 807 upper Selke (green) and the lower Selke (yellow) to nitrate export from the Selke catchment
 808 during low flow seasons (LFSs, yellow background) and high flow seasons (HFSs, blue
 809 background). Note that nitrate export from the lower Selke always is an integrated signal from
 810 the entire catchment. Subfigure a) shows the Selke catchment with its land use, its relative N
 811 input (not true to scale) and effective travel times of nitrate (TTs), b) shows the seasonal and
 812 event dynamics of nitrate export and c) the long-term CQ-relationships. Note that long-term CQ-
 813 relationships, as depicted in c) do not account for temporal shifts but represent the integrated
 814 signal.
 815

816 Water quality managers should be aware of these potential differences between sub-
817 catchments. If the aim is to reduce high nitrate loads, the focus must be on the upstream sub-
818 catchments with short TTDs and dynamic transport patterns. As nitrate concentrations are
819 especially high during winter and spring, an application of nitrate fixing crops during these
820 seasons is a promising measure to reduce nitrate leaching (Askegaard et al. 2005, Constantin et
821 al. 2009). Furthermore, large buffer stripes (> 50m) can decrease connectivity between
822 agricultural fields and the stream network (Mayer et al., 2005). Unfortunately, high N loading via
823 atmospheric deposition, as apparent in the Harz Mountains (Kuhr et al., 2014) cannot be
824 addressed on site but would require a large-scale reduction of fertilizer application and fossil fuel
825 combustion. Nevertheless, a substantial reduction of N-surplus from agriculture and measures to
826 decrease nitrate leaching are believed to have the potential for a significant and relatively fast
827 reduction of nitrate export to the streams, as the riverine concentration decrease after 1990
828 suggests.

829 If the aim is to reduce low flow nitrate concentrations to protect drinking water resources
830 and aquatic ecosystems on the long-term, lowland areas with extensive agricultural land use and
831 long TTs need to be the target for remediation measures. However, long TTs and legacy stores
832 will impede a fast success of nitrate reduction measures and will likely affect drinking water
833 quality and low-flow instream concentrations for years to come. For such groundwater-
834 dominated systems, long-term management strategies to reduce fertilizer application at a large
835 scale will be needed to effectively address nitrate pollution (Bieroza et al., 2018; Ehrhardt et al.,
836 2019).

837 In any case, to address short-term *and* long-term nitrate pollution, water quality managers
838 should neither solely focus on upstream areas of catchments nor solely on the lowland areas
839 where most of the agricultural land use typically occurs. Instead, they need to integrate all
840 characteristic landscape units and their interaction.

841 **5 Conclusions**

842 A key goal of this study was to characterize the spatial variability in nitrate export
843 dynamics across nested sub-catchments and to disentangle their respective contributions to the
844 integrated signal of nitrate export at the catchment outlet. Taking advantage of a comprehensive
845 dataset that includes long-term and high-frequency data from three nested sub-catchments in the
846 Selke catchment, we could show that sub-catchments can have very different nitrate export
847 dynamics that lead to seasonally different sub-catchment contributions to nitrate concentrations
848 and loads. The mountainous upstream part of the catchment (here the upper Selke) transports
849 temporally elevated nitrate concentrations during HFSs and events and has therefore a
850 disproportional contribution to nitrate loads. This imbalance underlines the important role of
851 upstream sub-catchments for effective measures to reduce nitrate pollution. Hence, nitrate export
852 from hydrologically responsive upstream catchments can be a serious threat to water quality,
853 especially with respect to exported loads. At the same time, short TTs emphasize a fast response
854 to changes in N input and dedicated mitigation measures are likely to show effects relatively
855 quickly. In contrast, lowland sub-catchments with long TTs and a dominance of agricultural land
856 use (here the lower Selke) pose a long-term and persistent problem of nitrate pollution, which
857 can threaten the quality of drinking water for decades. Nitrate export from these sub-catchments
858 is relatively steady and dominates during LFSs and base flow conditions. Its impact on nitrate
859 concentrations during HFSs and events and especially on nitrate loads, however, might be

860 overestimated if neglecting the impact from upstream sub-catchments. We do not aim at
861 prioritizing individual measures to reduce nitrate pollution between sub catchments, but we
862 emphasize the importance of sub-catchment-specific characteristics in order to place nitrate
863 reduction measures most effectively and to assume realistic timescales for their success.

864 We could further show that CQ-relationships for nitrate concentrations can change as a
865 reaction to changes in N input. While chemodynamic patterns can indicate ‘not equilibrated
866 systems’ that are still in transition towards a new equilibrium, chemostasis can indicate
867 homogeneously distributed N sources - both vertically in the subsurface and between sub-
868 catchments – after a prolonged period of stable N inputs. To detect these changes, it is crucial to
869 account for temporal changes and seasonality in CQ-relationships. Furthermore, we found that
870 the combined analyses of long-term trends and event scale CQ-slopes is a promising approach to
871 disentangle the impact from sub-catchments on nitrate export at the catchment outlet as it can
872 reveal short-term impacts from more dynamic upstream catchment export that is relevant for
873 load estimations and a more precise detection of N sources. Examining the whole range of time
874 scales – from long-term trends to the event scale – is therefore crucial to assess the full range of
875 sub-catchment impacts on nitrate export, as the times and time scales relevant for nitrate export
876 can vary substantially between sub-catchments.

877 Findings from this study should be further tested by applying our or similar approaches to
878 other mesoscale catchments with different characteristics and in different settings. Including the
879 knowledge gained from such studies on sub-catchment contributions to nitrate export into
880 spatially distributed water quality models would eventually lead to more precise projections and,
881 in turn, to more robust management strategies for water quality.

882 **Acknowledgments, Samples, and Data**

883 Funding for this study was provided by the DFG collaborative research center (SFB) 1253
884 “CAMPOS” as well as by the Helmholtz Research Program, Integrated Project “Water and
885 Matter Flux Dynamics in Catchments”. We cordially thank the State Office of Flood Protection
886 and Water Quality of Saxony-Anhalt (LHW) for providing discharge and nitrate concentration
887 data and to the Ministry of Environment, Agriculture and Energy Saxony-Anhalt (MULE) for the
888 provision of WWTP data. Furthermore, we would like to thank Martin Bach from the University
889 of Gießen for supplying N input data from agricultural areas and the MET Norway, for supplying
890 data to simulate atmospheric deposition. We thank Michael Rode for the provision of high-
891 frequency data from TERENO observational facilities and the German Meteorological Service
892 for the provision of meteorological datasets. Additionally we thank Florian Schnabel for
893 brainstorming on the conceptual framework and Kathrin Kuehnhammer and Samuel Mayer for
894 their valuable input to R codes for event separation.

895 Data availability:

896 Supplementary figures and tables are available as Supplementary Information. Datasets on i) FN
897 and non-FN nitrate concentrations, loads and CQ-slopes, ii) N input and iii) event characteristics
898 are available under: doi:10.4211/hs.c3ea08faa88a46a4a3ce596a09686198.

899 Raw data on discharge and water quality is freely available on the website of the State Office of
900 Flood Protection and Water Quality of Saxony-Anhalt (LHW), from gldweb.dhi-wasy.com/gld-portal/.

902
903 High frequency data of nitrate concentrations are archived in the TERENO data base and will
904 be available upon request through the TERENO-Portal (www.tereno.net/ddp).

905 Atmospheric deposition data can be accessed on the website of the Meteorological Synthesizing
906 Centre – West (MSC-W) of the European Monitoring and Evaluation Programm (EMEP)
907 (http://emep.int/mscw/index_mscw.html, Norwegian Meteorological Institute, 2017), which is
908 assigned to the Meteorological Institute of BNorway (MET Norway).

909 The raw meteorological datasets can be obtained freely from German Weather Service (DWD);
910 and gridded products based on Zink et al. (2017) from <https://www.ufz.de/index.php?en=41160>
911

912 **References**

- 913 Alexander, R. B., Boyer, E. W., Smith, R. A., Schwarz, G. E., & Moore, R. B. (2007).
914 The role of headwater streams in downstream water quality 1. *JAWRA Journal of the American*
915 *Water Resources Association*, 43(1), 41–59, doi:10.1111/j.1752-1688.2007.00005.x
- 916 Bach, M., & Frede, H.-G. (1998). Agricultural nitrogen, phosphorus and potassium
917 balances in Germany—methodology and trends 1970 to 1995. *Zeitschrift Für Pflanzenernährung*
918 *Und Bodenkunde*, 161(4), 385–393, doi:10.1002/jpln.1998.3581610406
- 919 Bach, M., Breuer, L., Frede, H.-G., Huisman, J. A., & Otte, A. (2006). Accuracy and
920 congruency of three different digital land-use maps. *Landscape and Urban Planning*, 78(4),
921 289–299, doi:10.1016/j.landurbplan.2005.09.004
- 922 Bartnicky, J., & Benedictow, A. (2017). Atmospheric Deposition of Nitrogen to OSPAR
923 Convention waters in the period 1995–2014. *EMEP MSC-W Report for OSPAR EMEP/MSW*
924 *Technical Report, 1*.
- 925 Bartnicky, Jerzy, & Fagerli, H. (2004). *Atmospheric Nitrogen in the OSPAR Convention*
926 *Area in the Period 1990–2004. Summary Report for the OSPAR Convention*. EMEP Technical
927 Report MSC-W 4/2006. Norwegian Meteorological Institute, Oslo
- 928 Basu, N. B., Destouni, G., Jawitz, J. W., Thompson, S. E., Loukinova, N. V., Darracq,
929 A., et al. (2010). Nutrient loads exported from managed catchments reveal emergent
930 biogeochemical stationarity. *Geophysical Research Letters*, 37(23), doi:10.1029/2010GL045168
- 931 Basu, N. B., Thompson, S. E., & Rao, P. S. C. (2011). Hydrologic and biogeochemical
932 functioning of intensively managed catchments: A synthesis of top-down analyses. *Water*
933 *Resources Research*, 47(10), doi:10.1029/2011WR010800
- 934 Bernal, S., Butturini, A., & Sabater, F. (2002). Variability of DOC and nitrate responses
935 to storms in a small Mediterranean forested catchment. *Hydrology and Earth System Sciences*
936 *Discussions*, 6(6), 1031–1041.
- 937 Bieroza, M. Z., Heathwaite, A. L., Bechmann, M., Kyllmar, K., & Jordan, P. (2018). The
938 concentration-discharge slope as a tool for water quality management. *Science of the Total*
939 *Environment*, 630, 738–749, doi:10.1016/j.scitotenv.2018.02.256

- 940 Blöschl, G., Bierkens, M. F., Chambel, A., Cudennec, C., Destouni, G., Fiori, A., et al.
941 (2019). Twenty-three Unsolved Problems in Hydrology (UPH)—a community perspective.
942 *Hydrological Sciences Journal*, 64(10), 1141–1158, doi:10.1080/02626667.2019.1620507
- 943 Bouraoui, F., & Grizzetti, B. (2011). Long term change of nutrient concentrations of
944 rivers discharging in European seas. *Science of the Total Environment*, 409(23), 4899–4916,
945 doi:10.1016/j.scitotenv.2011.08.015
- 946 Bowes, M. J., Jarvie, H. P., Halliday, S. J., Skeffington, R. A., Wade, A. J., Loewenthal,
947 M., et al. (2015). Characterising phosphorus and nitrate inputs to a rural river using high-
948 frequency concentration–flow relationships. *Science of the Total Environment*, 511, 608–620,
949 doi:10.1016/j.scitotenv.2014.12.086
- 950 Breuer, L., Vache, K. B., Julich, S., & Frede, H.-G. (2008). Current concepts in nitrogen
951 dynamics for mesoscale catchments. *Hydrological Sciences Journal*, 53(5), 1059–1074,
952 doi:10.1623/hysj.53.5.1059
- 953 Burns, D. A., Pellerin, B. A., Miller, M. P., Capel, P. D., Tesoriero, A. J., & Duncan, J.
954 M. (2019). Monitoring the riverine pulse: Applying high-frequency nitrate data to advance
955 integrative understanding of biogeochemical and hydrological processes. *Wiley Interdisciplinary*
956 *Reviews: Water*, e1348, doi:10.1002/wat2.1348
- 957 Camargo, J. A., & Alonso, Á. (2006). Ecological and toxicological effects of inorganic
958 nitrogen pollution in aquatic ecosystems: a global assessment. *Environment International*, 32(6),
959 831–849, doi:10.1016/j.envint.2006.05.002
- 960 Caraco, N. F., & Cole, J. J. (1999). Human impact on nitrate export: an analysis using
961 major world rivers. *Ambio*, 28(2), 167–170.
- 962 Dodds, W. K., & Oakes, R. M. (2008). Headwater Influences on Downstream Water
963 Quality. *Environmental Management*, 41(3), 367–377, doi:10.1007/s00267-007-9033-y
- 964 Duncan, J. M., Welty, C., Kemper, J. T., Groffman, P. M., & Band, L. E. (2017).
965 Dynamics of nitrate concentration-discharge patterns in an urban watershed. *Water Resources*
966 *Research*, 53(8), 7349–7365, doi:10.1002/2017WR020500
- 967 Dupas, R., Jomaa, S., Musolff, A., Borchardt, D., & Rode, M. (2016). Disentangling the
968 influence of hydroclimatic patterns and agricultural management on river nitrate dynamics from
969 sub-hourly to decadal time scales. *Science of the Total Environment*, 571, 791–800,
970 doi:10.1016/j.scitotenv.2016.07.053
- 971 Dupas, R., Musolff, A., Jawitz, J. W., Rao, P. S. C., Jäger, C. G., Fleckenstein, J. H., et
972 al. (2017). Carbon and nutrient export regimes from headwater catchments to downstream
973 reaches. *Biogeosciences*, 14(18), 4391–4407, doi:10.5194/bg-14-4391-2017
- 974 Dupas, R., Abbott, B. W., Minaudo, C., & Fovet, O. (2019). Distribution of landscape
975 units within catchments influences nutrient export dynamics. *Frontiers in Environmental*
976 *Science*, 7, 43, doi:10.3389/fenvs.2019.00043
- 977 Eder, A., Strauss, P., Krueger, T., & Quinton, J. N. (2010). Comparative calculation of
978 suspended sediment loads with respect to hysteresis effects (in the Petzenkirchen catchment,
979 Austria). *Journal of Hydrology*, 389(1), 168–176, doi:10.1016/j.jhydrol.2010.05.043

- 980 EEA, (European Environment Agency). (2012). Corine Land COVer. European
981 Environment Agency, Copenhagen. Retrieved from [https://land.copernicus.eu/pan-](https://land.copernicus.eu/pan-european/corine-land-cover)
982 [european/corine-land-cover](https://land.copernicus.eu/pan-european/corine-land-cover)
- 983 Ehrhardt, S., Kumar, R., Fleckenstein, J. H., Attinger, S., & Musolff, A. (2019).
984 Trajectories of nitrate input and output in three nested catchments along a land use gradient.
985 *Hydrology and Earth System Sciences*, 23(9), 3503–3524.
- 986 Godsey, S. E., Kirchner, J. W., & Clow, D. W. (2009). Concentration–discharge
987 relationships reflect chemostatic characteristics of US catchments. *Hydrological Processes*,
988 23(13), 1844–1864, doi:10.1002/hyp.7315
- 989 Goodridge, B. M., & Melack, J. M. (2012). Land use control of stream nitrate
990 concentrations in mountainous coastal California watersheds. *Journal of Geophysical Research:*
991 *Biogeosciences*, 117(G2).
- 992 Gross, N. (1996). Farming in former East Germany: Past policies and future prospects.
993 *Landscape and Urban Planning*, 35(1), 25–40, doi:10.1016/0169-2046(95)00215-4
- 994 Gustard, A. (1983). Regional variability of soil characteristics for flood and low flow
995 estimation. *Agricultural Water Management*, 6(2–3), 255–268.
- 996 Hannappel, S., Köpp, C., & Bach, T. (2018). Charakterisierung des
997 Nitratabbauvermögens der Grundwasserleiter in Sachsen-Anhalt. *Grundwasser*, 23(4), 311–321.
- 998 Häußermann, U., Bach, M., Klement, L., & Breuer, L. (2019). Stickstoff-Flächenbilanzen
999 für Deutschland mit Regionalgliederung Bundesländer und Kreise - Jahre 1995 bis 2017
1000 Methodik, Ergebnisse und Minderungsmaßnahmen. Umweltbundesamt. Retrieved from
1001 [https://www.umweltbundesamt.de/sites/default/files/medien/1410/publikationen/2019-10-](https://www.umweltbundesamt.de/sites/default/files/medien/1410/publikationen/2019-10-28_texte_131-2019_stickstoffflaechenbilanz.pdf)
1002 [28_texte_131-2019_stickstoffflaechenbilanz.pdf](https://www.umweltbundesamt.de/sites/default/files/medien/1410/publikationen/2019-10-28_texte_131-2019_stickstoffflaechenbilanz.pdf)
- 1003 Hirsch, R. M., Moyer, D. L., & Archfield, S. A. (2010). Weighted regressions on time,
1004 discharge, and season (WRTDS), with an application to Chesapeake Bay river inputs 1. *JAWRA*
1005 *Journal of the American Water Resources Association*, 46(5), 857–880, doi:10.1111/j.1752-
1006 1688.2010.00482.x
- 1007 Hirsch, R. M., Archfield, S. A., & De Cicco, L. A. (2015). A bootstrap method for
1008 estimating uncertainty of water quality trends. *Environmental Modelling & Software*, 73, 148–
1009 166, doi:10.1016/j.envsoft.2015.07.017
- 1010 Hrachowitz, M., Soulsby, C., Tetzlaff, D., Dawson, J. J. C., Dunn, S. M., & Malcolm, I.
1011 A. (2009). Using long-term data sets to understand transit times in contrasting headwater
1012 catchments. *Journal of Hydrology*, 367(3), 237–248, doi:10.1016/j.jhydrol.2009.01.001
- 1013 Inamdar, S. P., O’leary, N., Mitchell, M. J., & Riley, J. T. (2006). The impact of storm
1014 events on solute exports from a glaciated forested watershed in western New York, USA.
1015 *Hydrological Processes: An International Journal*, 20(16), 3423–3439, doi:10.1002/hyp.6141
- 1016 Jawitz, J. W., & Mitchell, J. (2011). Temporal inequality in catchment discharge and
1017 solute export. *Water Resources Research*, 47(10), doi:10.1029/2010WR010197
- 1018 Jiang, S., Jomaa, S., & Rode, M. (2014). Modelling inorganic nitrogen leaching in nested
1019 mesoscale catchments in central Germany. *Ecohydrology*, 7(5), 1345–1362,
1020 doi:10.1002/eco.1462

- 1021 Kohl, D. H., Shearer, G. B., & Commoner, B. (1971). Fertilizer nitrogen: contribution to
1022 nitrate in surface water in a corn belt watershed. *Science*, *174*(4016), 1331–1334, doi:
1023 10.1126/science.174.4016.1331
- 1024 Köhne, C., & Wendland, F. (1992). *Modellgestützte Berechnung des mikrobiellen*
1025 *Nitratabbaus im Boden*. KFA.
- 1026 Krause, P., Bäse, F., Bende-Michl, U., Fink, M., Flügel, W., & Pfennig, B. (2006).
1027 Multiscale investigations in a mesoscale catchment? hydrological modelling in the Gera
1028 catchment.
- 1029 Krueger, T., Quinton, J. N., Freer, J., Macleod, C. J. A., Bilotta, G. S., Brazier, R. E., et
1030 al. (2009). Uncertainties in Data and Models to Describe Event Dynamics of Agricultural
1031 Sediment and Phosphorus Transfer. *Journal of Environmental Quality*, *38*(3), 1137–1148,
1032 doi:10.2134/jeq2008.0179
- 1033 Kuhr, P., Kunkel, R., Tetzlaff, B., & Wendland, F. (2014). Räumlich differenzierte
1034 Quantifizierung der Nährstoffeinträge in Grundwasser und Oberflächengewässer in Sachsen-
1035 Anhalt unter Anwendung der Modellkombination GROWA-WEKU-MEPhos. *FZ Jülich*,
1036 *Endbericht Vom*, *25*, 2014.
- 1037 Kunkel, R., & Wendland, F. (2006). Diffuse Nitrateinträge in die Grund-und
1038 Oberflächengewässer von Rhein und Ems. *Forschungszentrum Jülich GmbH, Jülich, Germany*.
- 1039 Lutz, S. R., Trauth, N., Musolff, A., Van Breukelen, B. M., Knöller, K., & Fleckenstein,
1040 J. H. (2020). How Important is Denitrification in Riparian Zones? Combining End-Member
1041 Mixing and Isotope Modeling to Quantify Nitrate Removal from Riparian Groundwater. *Water*
1042 *Resources Research*, *56*(1), e2019WR025528, doi:10.1029/2019WR025528
- 1043 Majumdar, D., & Gupta, N. (2000). Nitrate pollution of groundwater and associated
1044 human health disorders. *Indian Journal of Environmental Health*, *42*(1), 28–39.
- 1045 Mayer, P. M., Reynolds, S. K., McCutchen, M. D., & Canfield, T. J. (2005). Riparian
1046 buffer width, vegetative cover, and nitrogen removal effectiveness: A review of current science
1047 and regulations. *US Environmental Protection Agency*, *27*.
- 1048 McLenaghan, R. D., Cameron, K. C., Lampkin, N. H., Daly, M. L., & Deo, B. (1996).
1049 Nitrate leaching from ploughed pasture and the effectiveness of winter catch crops in reducing
1050 leaching losses. *New Zealand Journal of Agricultural Research*, *39*(3), 413–420,
1051 doi:10.1080/00288233.1996.9513202
- 1052 Minaudo, C., Dupas, R., Gascuel-Oudou, C., Fovet, O., Mellander, P.-E., Jordan, P., et al.
1053 (2017). Nonlinear empirical modeling to estimate phosphorus exports using continuous records
1054 of turbidity and discharge. *Water Resources Research*, *53*(9), 7590–7606,
1055 doi:10.1002/2017WR020590
- 1056 Montzka, C., Canty, M., Kunkel, R., Menz, G., Vereecken, H., & Wendland, F. (2008).
1057 Modelling the water balance of a mesoscale catchment basin using remotely sensed land cover
1058 data. *Journal of Hydrology*, *353*(3–4), 322–334. doi: 10.1016/j.jhydrol.2008.02.018
- 1059 Musolff, A., Fleckenstein, J. H., Rao, P. S. C., & Jawitz, J. W. (2017). Emergent
1060 archetype patterns of coupled hydrologic and biogeochemical responses in catchments.
1061 *Geophysical Research Letters*, *44*(9), 4143–4151, doi:10.1002/2017GL072630

- 1062 Musolff, A., Schmidt, C., Selle, B., & Fleckenstein, J. H. (2015). Catchment controls on
1063 solute export. *Advances in Water Resources*, *86*, 133–146, doi: 10.1016/j.advwatres.2015.09.026
- 1064 Musolff, A., Schmidt, C., Rode, M., Lischeid, G., Weise, S. M., & Fleckenstein, J. H.
1065 (2016). Groundwater head controls nitrate export from an agricultural lowland catchment.
1066 *Advances in Water Resources*, *96*, 95–107, doi:10.1016/j.advwatres.2016.07.003
- 1067 Padilla, F. M., Gallardo, M., & Manzano-Agugliaro, F. (2018). Global trends in nitrate
1068 leaching research in the 1960–2017 period. *Science of the Total Environment*, *643*, 400–413, doi:
1069 10.1016/j.scitotenv.2018.06.215
- 1070 R Core Team. (2019). *R: A language and environment for statistical computing*. Vienna,
1071 Austria. Retrieved from <https://www.R-project.org/>
- 1072 Rockström, J., Steffen, W., Noone, K., Persson, Å., Chapin III, F. S., Lambin, E. F., et al.
1073 (2009). A safe operating space for humanity. *Nature*, *461*(7263), 472.
- 1074 Rode, M., Halbedel née Angelstein, S., Anis, M. R., Borchardt, D., & Weitere, M.
1075 (2016). Continuous in-stream assimilatory nitrate uptake from high-frequency sensor
1076 measurements. *Environmental Science & Technology*, *50*(11), 5685–5694,
1077 doi:10.1021/acs.est.6b00943
- 1078 Rose, L. A., Karwan, D. L., & Godsey, S. E. (2018). Concentration–discharge
1079 relationships describe solute and sediment mobilization, reaction, and transport at event and
1080 longer timescales. *Hydrological Processes*, *32*(18), 2829–2844, doi:10.1002/hyp.13235
- 1081 Seitzinger, S., Harrison, J. A., Böhlke, J. K., Bouwman, A. F., Lowrance, R., Peterson,
1082 B., et al. (2006). Denitrification across landscapes and waterscapes: a synthesis. *Ecological*
1083 *Applications*, *16*(6), 2064–2090, doi:10.1890/1051-0761(2006)016[2064:DALAWA]2.0.CO;2
- 1084 Silva, S. R., Ging, P. B., Lee, R. W., Ebbert, J. C., Tesoriero, A. J., & Inkpen, E. L.
1085 (2002). Forensic applications of nitrogen and oxygen isotopes in tracing nitrate sources in urban
1086 environments. *Environmental Forensics*, *3*(2), 125–130.
- 1087 Soulsby, C., Birkel, C., Geris, J., Dick, J., Tunaley, C., & Tetzlaff, D. (2015). Stream
1088 water age distributions controlled by storage dynamics and nonlinear hydrologic connectivity:
1089 Modeling with high-resolution isotope data. *Water Resources Research*, *51*(9), 7759–7776, doi:
1090 10.1002/2015WR017888
- 1091 Strebel, O., Duynisveld, W. H. M., & Böttcher, J. (1989). Nitrate pollution of
1092 groundwater in western Europe. *Agriculture, Ecosystems & Environment*, *26*(3–4), 189–214, doi:
1093 10.1016/0167-8809(89)90013-3
- 1094 Tarasova, L., Basso, S., Zink, M., & Merz, R. (2018). Exploring Controls on Rainfall-
1095 Runoff Events: 1. Time Series-Based Event Separation and Temporal Dynamics of Event Runoff
1096 Response in Germany. *Water Resources Research*, *54*(10), 7711–7732, doi:
1097 10.1029/2018WR022587
- 1098 Thompson, S. E., Basu, N. B., Lascurain, J., Aubeneau, A., & Rao, P. S. C. (2011).
1099 Relative dominance of hydrologic versus biogeochemical factors on solute export across impact
1100 gradients. *Water Resources Research*, *47*(10), doi:10.1029/2010WR009605

- 1101 Trauth, N., Musolff, A., Knöller, K., Kaden, U. S., Keller, T., Werban, U., &
1102 Fleckenstein, J. H. (2018). River water infiltration enhances denitrification efficiency in riparian
1103 groundwater. *Water Research*, *130*, 185–199, doi:10.1016/j.watres.2017.11.058
- 1104 Tuckey, J. W. (1977). *Exploratory Data Analysis*. 1977. *Mass: Addison-Wesley*
1105 *Publishing Company Reading*.
- 1106 Van Meter, K J, & Basu, N. B. (2017). Time lags in watershed-scale nutrient transport:
1107 an exploration of dominant controls. *Environmental Research Letters*, *12*(8), 084017,
1108 doi:10.1088/1748-9326/aa7bf4
- 1109 Van Meter, K. J., Basu, N. B., & Van Cappellen, P. (2017). Two centuries of nitrogen
1110 dynamics: Legacy sources and sinks in the Mississippi and Susquehanna River Basins. *Global*
1111 *Biogeochemical Cycles*, *31*(1), 2–23, doi:10.1002/2016GB005498
- 1112 Van Meter, Kimberly J., Basu, N. B., Veenstra, J. J., & Burras, C. L. (2016). The
1113 nitrogen legacy: emerging evidence of nitrogen accumulation in anthropogenic landscapes.
1114 *Environmental Research Letters*, *11*(3), 035014, doi:10.1088/1748-9326/11/3/035014
- 1115 Whitehead, P. G., Wilby, R. L., Battarbee, R. W., Kernan, M., & Wade, A. J. (2009). A
1116 review of the potential impacts of climate change on surface water quality. *Hydrological*
1117 *Sciences Journal*, *54*(1), 101–123, doi:10.1623/hysj.54.1.101
- 1118 WMO. (2008). *Manual on low-flow estimation and prediction*. Geneva: World
1119 Meteorological Organization (Geneva).
- 1120 Wollschläger, U., Attinger, S., Borchardt, D., Brauns, M., Cuntz, M., Dietrich, P., et al.
1121 (2017). The Bode hydrological observatory: a platform for integrated, interdisciplinary hydro-
1122 ecological research within the TERENO Harz/Central German Lowland Observatory.
1123 *Environmental Earth Sciences*, *76*(1), 29, doi:10.1007/s12665-016-6327-5
- 1124 Yang, J., Heidbüchel, I., Musolff, A., Reinstorf, F., & Fleckenstein, J. H. (2018).
1125 Exploring the dynamics of transit times and subsurface mixing in a small agricultural catchment.
1126 *Water Resources Research*, *54*(3), 2317–2335, doi:10.1002/2017WR021896
- 1127 Yang, X., Jomaa, S., Zink, M., Fleckenstein, J. H., Borchardt, D., & Rode, M. (2018). A
1128 New Fully Distributed Model of Nitrate Transport and Removal at Catchment Scale. *Water*
1129 *Resources Research*, *54*(8), 5856–5877, doi:10.1029/2017WR022380
- 1130 Zhang, Q., Harman, C. J., & Ball, W. P. (2016). An improved method for interpretation
1131 of riverine concentration-discharge relationships indicates long-term shifts in reservoir sediment
1132 trapping. *Geophysical Research Letters*, *43*(19), doi:10.1002/2016GL069945
- 1133 Zink, M., Kumar, R., Cuntz, M., & Samaniego, L. (2017). A high-resolution dataset of
1134 water fluxes and states for Germany accounting for parametric uncertainty, doi:10.5194/hess-21-
1135 1769-2017
- 1136